AN ABSTRACT OF THE THESIS OF

JACK ALAN MITCHELL for the M. S. in Mechanical Engineering
                                    (Degree)   (Major)

Date thesis is presented _____October 7, 1963_____

Title CONTROL OF PEAK STRESSES IN TENSILE TESTING

MACHINE COMPONENTS SUBJECTED TO SHOCK LOADING

Abstract approved ████████████████████████████
                         (Major professor)

The mechanical properties of materials at cryogenic tempera-

tures have been the subject of increasing interest during the past few

years, although very little actual materials testing has been done at

extremely low temperatures because of the high cost and low heat of

vaporaization of liquid helium. Recently, the Department of

Mechanical and Industrial Engineering at Oregon State University

initiated a research program of materials testing at liquid helium

temperatures, 4.2° K. A specially designed cryogenic tensile testing

machine has been built employing a variable rate of loading and an

electronic chart drive recorder.

A Baldwin U-1 load cell was placed in the loading column of

the testing machine to measure the magnitude of the applied load. Pre-

vious experience has found that damage to the load cell can occur because

of the shock environment present upon fracture of a tensile specimen.

The object of this thesis is to analyze the effects of shock loading on the cryogenic tensile testing machine and to develop a means of reducing any shock environment seen by the load cell.

After determining that 92.6 percent of the strain energy in the loading column was stored in the tensile rod between the load cell and tensile specimen, a theoretical analysis of the response of the tensile rod and load cell to specimen fracture was made using the mathematical model of a long, slender rod with fixed-free end conditions and a suddenly removed axial load. The theoretical fundamental frequencies of the tensile rod and load cell were found to be 1570 and 5940 cycles per second, respectively.

In order to verify the problem of a shock environment imposed on the load cell and to check the theoretical results, an experimental study of the actual system was made. Strain gages on the tensile rod, on the adapter above the load cell, and in the load cell measured the motion response of these components to specimen fracture at room temperature. An oscilloscope and camera were used to record the results. The actual fundamental frequencies of the tensile rod and load cell were 1080 and 3250 cycles per second, respectively, and the assumed problem of shock environment on the load cell was verified.

After studying many methods of absorbing and damping the shock loading, it was decided to design and fabricate a shock

absorber having a piston and cylinder arrangement with a shock absorbing medium placed between the piston and cylinder head. Polyethylene and polyester urethane foams were chosen as possible shock absorbing mediums because of their excellent energy dissipation properties in compression.

After the shock absorber was fabricated and placed in the testing machine, its effectiveness was determined by following the experimental procedures previously used. Results indicated that the initial load release was adequately damped with polyethylene foam. Less damping was noticed with the polyester foam. In both cases, however, a delayed peak compressive force on the load cell occurred three milliseconds after specimen fracture. When it was determined that this force was due to the motion of the top plate of the testing machine, the jack on the top plate was spring mounted. Test results of this system showed that the maximum peak compressive force following specimen fracture was reduced to 15 percent of the tensile force before fracture when polyethylene foam was used as the shock absorbing medium; however, when the polyester foam was used, the test results indicated that the foam bottomed out. Polyethylene foam thus proved to be a substantially superior solution to the problem under consideration.

CONTROL OF PEAK STRESSES
IN TENSILE TESTING MACHINE COMPONENTS
SUBJECTED TO SHOCK LOADING

by
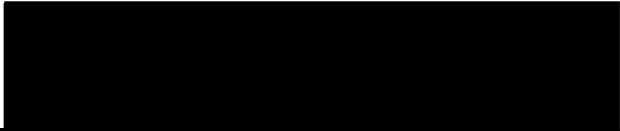
JACK ALAN MITCHELL

A THESIS

submitted to

OREGON STATE UNIVERSITY

in partial fulfillment of
the requirements for the
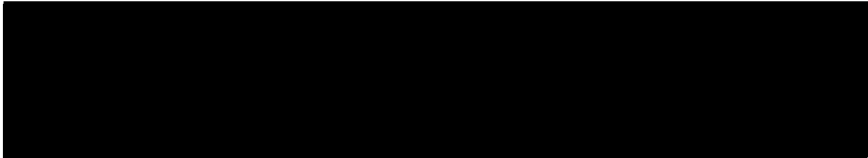degree of

MASTER OF SCIENCE

June 1964

APPROVED:

<div style="text-align:center">████████████████</div>

Associate Professor of Mechanical Engineering

In Charge of Major

<div style="text-align:center">████████████████</div>

Head of Department, Mechanical and Industrial
Engineering

<div style="text-align:center">████████████████</div>

Dean of Graduate School

Date thesis is presented _October 7, 1963_

Typed by Illa W. Atwood

ACKNOWLEDGEMENTS

TABLE OF CONTENTS

LIST OF FIGURES

LIST OF TABLES

NOMENCLATURE

A   = area, inches

b   = flange thickness, inches

c   = $\sqrt{E/\rho}$ = velocity of wave propagation, inches per second

C, D   = constants of integration

d   = weld thickness, inches

E   = modulus of elasticity, pounds per square inch

f   = frequency, cycles per second

F, G   = constants of integration

h   = thickness of foam material, inches

i   = positive integer

L   = length of tensile rod, inches

M   = torque, inch-pounds

n   = positive integer

P   = axial force, pounds

R(x)   = function of x

S(t)   = function of t

t   = time, seconds

T   = load reduction factor

u(x, t)   = longitudinal displacement of tensile rod, inches

U   = energy capacity of shock absorbing medium, inch-pounds per cubic inch

V	=	volume, cubic inches
W	=	strain energy, inch-pounds
x	=	axial space coordinate
y	=	deflection, inches
β	=	$2\pi f$ = angular frequency, radians per second
ϵ	=	strain, inches per inch
ρ	=	mass density of rod, pound seconds squared per inches to the fourth power
σ	=	normal stress, pounds per square inch
σ_s	=	shear stress, pounds per square inch

INTRODUCTION

The mechanical properties of materials at cryogenic tempera-
tures have been the subject of extensive interest during the past few
years, and several laboratories have been actively engaged in mater-
ials research and testing at these temperatures. The majority of
this work, however, has been done in the temperature ranges of
liquid oxygen, nitrogen, and hydrogen. The transfer and storage
boil-off rates of these liquefied gases are not excessive and their
liquefaction costs are low.

Very little actual materials testing has been done at lower
temperatures using liquid helium because its heat of vaporization is
extremely low when compared to that of liquid oxygen, nitrogen, and
hydrogen, and its liquefaction cost is high enough to prohibit or
greatly hinder its use in the majority of materials testing programs.
Most researchers, instead, have extrapolated their data from the
known materials properties at higher temperatures.

Recently, the Department of Mechanical and Industrial
Engineering at Oregon State University decided to inaugurate a
research program of materials testing at cryogenic temperatures,
with an emphasis on temperatures in the region of liquid helium.
The actual development of the program began when Carl Fullman
wrote a Master's thesis on "The Design of a Mechanism for Tensile

Testing in a Liquid Helium Dewar" (8). The object of his thesis was

to design a system for tensile testing at liquid helium temperatures

that would be inexpensive and efficient, and that would eliminate the

need of a local supply of liquid helium. Carl Fullman's design will

enable the research worker willing to make a modest investment to

carry on a tensile testing program at extremely low temperatures.

The main feature and advantage of the design is that it enables the

cryogenic liquid shipping container to be used as the testing chamber,

thus eliminating the drastic losses incurred when the liquid helium is

transferred to a separate cryostat.

The development of Oregon State University's low temperature

materials testing program was continued when Gordon Hull wrote his

Master's thesis on "The Design of a Variable Strain Rate, Auto-

graphic Recording, Tensile Testing Machine" (13). The purpose of

his thesis was to design a tensile testing machine that would be par-

ticularly adaptable for use with the apparatus designed by Carl

Fullman. The testing machine, shown in Figure 1, has a load capac-

ity of 20,000 pounds and a variable strain rate ranging from zero to

one inch per minute. A history of the entire load-deformation curve

is obtained by using a Honeywell-Brown Electronik chart recorder.

The load is measured through a Baldwin-Lima-Hamilton Type U-1

load cell and the deformation is obtained by a mechanical drive

Transmission

Jack

Top Plate

Vertical Support

Load Cell

Tensile Rod

Reaction Beam

Compression Column

Yoke Assembly

Specimen

Dewar

Dewar Rotation Assembly
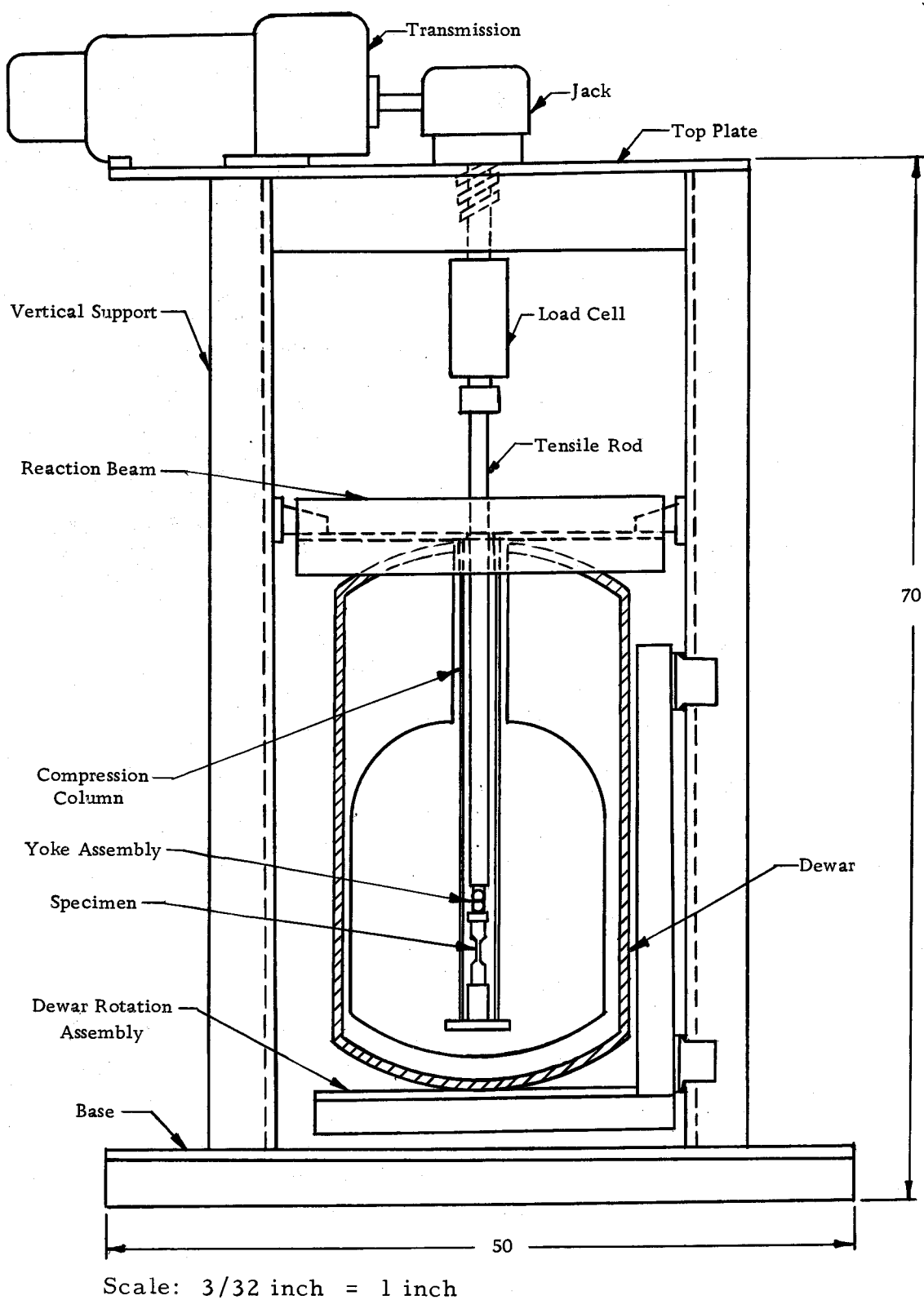
Base

70

50

Scale: 3/32 inch = 1 inch

Figure 1. Cryogenic tensile testing machine

connection between the jack and the chart-drive of the recorder.

This testing machine has been designed primarily for low temperature testing; however, since Oregon State University does not have a testing machine capable of recording a complete load-deformation curve, it was also designed so that tensile tests can be performed at room temperatures and elevated temperatures.

The Baldwin-Lima-Hamilton load cell used in the testing machine is essentially a resistance strain bridge having a structural configuration similar to that shown in Figure 2. The strain gage elements are bonded to the surface of the strain member.

It has been found from previous experience that, after using the load cell in a considerable number of tension tests and having it directly connected in the loading column, it will give inaccurate readings.[1] The apparent reason for this decrease in accuracy is that repeated shock loading of the load cell, which is thought to occur when the tensile specimen fractures, eventually causes the bonding between the strain gages and the strain member to fail. Since the load cell is one of the more expensive items in a testing machine and the validity of any test results depends on its accuracy, precautions

---

[1] Olleman, Roger D., Associate Professor of Mechanical Engineering, Oregon State University. Private communication. Corvallis, 1963.
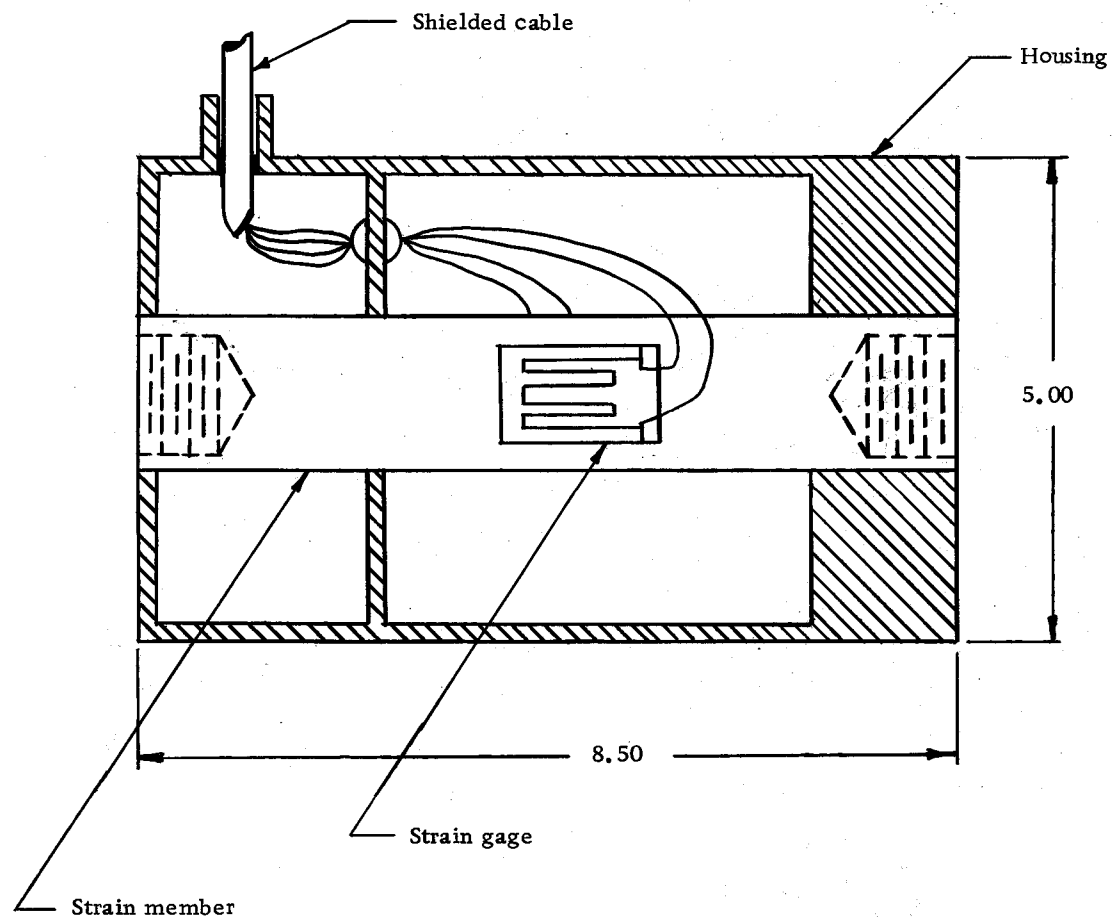
Figure 2. Baldwin type U-1 load cell

should be taken to protect the load cell from as much shock environment as possible.

The objective of this thesis is to analyze the system response to shock loading on the cryogenic tensile testing machine at Oregon State University and to develop a means of controlling any peak shock loads on the load cell.

THEORY AND ANALYSIS

An analysis of the system response to shock loads incurred when the specimen fractures must be made so that suitable design parameters for an energy dissipating device can be determined. Since all members of the testing machine are affected by the conditions of loading and unloading of the test specimen, the amount that each member contributes to the shock environment of the load cell must be found. One method of establishing their relative importance is to calculate the strain energy of each member of the system under maximum load.

Strain Energy of System

The strain energy of the system can be determined from the formula:

$$\text{Strain energy} = \frac{Py}{2}$$

where P is the load imposed on the system and y is the total deflection of all members in the system (12, p. 229).

The deflections of the members of the testing machine, under a load of 20,000 pounds, were calculated (see Appendix). The results of the calculations are as follows:

Member	Deflection
Top plate	0.0040 inches
Vertical supports	0.0010
Reaction beam attachments	0.0093
Reaction beam	0.0010
Jack screw (fully extended)	0.0028
Adapter	0.0018
Load cell	0.0050
Adapter	0.0018
Tensile rod	0.1565
Yoke assembly	0.0037
Tensile specimen (approximate)	0.0150
Compressive column	0.0426
Total	0.2465 inches

When a specimen fractures, the load cell will be affected primarily by the energy dissipated in the top plate, jack screw, tensile rod, yoke assembly, adapters, specimen, and the load cell itself. These members have a total deflection of 0.1856 inches, and their strain energy under the 20,000 pound load is 1856 inch-pounds. The tensile rod, tensile rod adapter, yoke assembly and specimen contain 1720 inch-pounds, or 92.6 percent of the strain energy acting upon the load cell. Therefore, these members constitute the critical area when determining the response of the system to the shock environment caused by specimen fracture, and the analysis of the thesis will be based on this premise.

Response of Tensile Rod

For the purpose of analysis it may be assumed that the tensile rod is rigidly attached to the load cell. The load cell, in turn, is rigidly mounted to the top plate of the testing machine. The effect of the jack screw in the following analysis is negligible and the adapter, yoke assembly and specimen are to be considered as an extension of the tensile rod.

Since the load cell and top plate are relatively stiff they may be assumed as rigid members with little error. Thus the problem to be solved will be that of a long, slender rod, fixed at its upper boundary and free at its lower boundary, as shown in Figure 3.
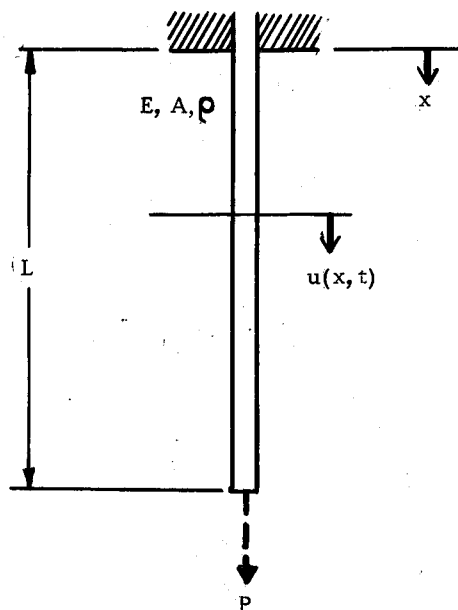

Figure 3. Longitudinally vibrating bar with fixed-free end conditions

The axial force, P, initially exists at the free end of the bar. When this force is suddenly removed, longitudinal vibrations are excited in the bar, and each increment of length in the bar is alternately compressed and extended. Since the bar is relatively slender, inertia forces in the lateral direction can be neglected. Plane cross-sections are assumed to remain plane so that internal forces in the bar are essentially axial.

The stress - strain relationship is assumed to obey Hooke's Law and, therefore, can be stated as:[2]

$$\sigma (x,t) = E \epsilon = E \frac{\partial u}{\partial x}$$

The governing differential equation of motion, assuming a constant cross-sectional area, is (22, p. 240):

$$\frac{\partial^2 u}{\partial t^2} = \frac{E}{\rho} \frac{\partial^2 u}{\partial x^2}$$

Since linear displacement along the longitudinal axis of the rod is the only space variable there can be only two independent boundary conditions. They are:

$$u(o,t) = 0 \qquad \text{(displacement at fixed end)}$$

and

$$E \left(\frac{\partial u}{\partial x} \right)_{x=L} = 0 \quad \text{(stress at free end)}$$

---

[2] Definitions for the symbols used in this thesis can be found in the Nomenclature.

The initial conditions, from the requirements stated previously, are:

$$u(x,o) = \epsilon x \qquad \text{(elongation along the x axis)}$$

and

$$\left(\frac{\partial u}{\partial t}\right)_{t=0} = 0 \qquad \text{(velocity of tensile rod)}.$$

Many authors of vibration textbooks, such as Timoshenko (21, p. 303) and Tong (22, p. 252), have included the solution to the differential equation in their textbooks. Therefore, only the basic steps leading up to the solution will be outlined below.

Using the separation of variables technique assume that the displacement, u(x, t), can be written as:

$$u(x,t) = R(x)S(t)$$

The differential equation becomes:

$$R\frac{\partial^2 S}{\partial t^2} = \frac{E}{\rho} S \frac{\partial^2 R}{\partial x^2}$$

Let $\dfrac{E}{\rho} = c^2$. Then the equation can be rewritten as:

$$\frac{\frac{\partial^2 S}{\partial t^2}}{S} = c^2 \frac{\frac{\partial^2 R}{\partial x^2}}{R} = \beta^2$$

where β is a constant which must be negative so that S(t) does not grow with time. Thus, the variables have been separated and can be written as the two following independent differential equations:

$$\frac{d^2R}{dx^2} + \frac{\beta^2}{c^2} R = 0$$

and

$$\frac{d^2S}{dt^2} + \beta^2 S = 0$$

The general solution to the first equation can be written as:

$$R(x) = F \cos \frac{\beta}{c} x + G \sin \frac{\beta}{c} x$$

To satisfy the boundary conditions it is found that:

$$F = 0$$

and

$$G \cos \frac{\beta}{c} L = 0$$

The second equation is the characteristic or frequency equation of the system, from which the frequencies of the natural modes of vibration can be calculated. Note that the coefficient, G, is indeterminant but can be assumed equal to unity (22, p. 253). The characteristic roots of the system, by satisfying the frequency equation, are of the form:

$$\frac{\beta_i}{c} = \frac{(2i - 1)\pi}{2L}$$

Taking $i = 1, 2, 3, \ldots$, the frequencies of the various modes of vibration can be found. For example, the frequency of the first, or fundamental, mode of vibration is:

$$f_1 = \frac{\beta_1}{2\pi} = \frac{c}{4L}$$

The solution to the second differential equation can also be written in trigonometric form as:

$$S(t) = C \cos \beta t + D \sin \beta t$$

The general solution for $u(x,t)$ then becomes:

$$u(x,t) = \sin \frac{\beta x}{c} [C \cos \beta t + D \sin \beta t]$$

Using the initial conditions the constants, C and D, can be determined. They are:

$$C_i = \frac{8 \epsilon L (-1)^{i-1}}{(2i-1)^2 \pi^2} \qquad \text{for} \qquad 1, 2, 3, \ldots$$

and

$$D_i = 0 \qquad \text{for} \qquad 1, 2, 3, \ldots$$

The complete series solution for $u(x,t)$, after substituting for C and β, is then:

$$u(x,t) = \frac{8 \epsilon L}{\pi^2} \sum_{i=1}^{\infty} \frac{(-1)^{i-1}}{(2i-1)^2} \sin \frac{(2i-1)\pi x}{2L} \cos \frac{(2i-1)\pi c t}{2L}$$

Returning to the assumption that:

$$\sigma(x,t) = E \frac{\partial u}{\partial x}$$

the theoretical stress distribution in the rod can be found at any instant during the period of vibration. Its equation is:

$$\sigma\left(x,t\right) = \frac{4E\epsilon}{\pi} \sum_{i=1}^{\infty} \frac{(-1)^{i-1}}{2i-1} \cos \frac{(2i-1)\pi x}{2L} \cos \frac{(2i-1)\pi ct}{2L}$$

The physical significance of the above equations for deflection and stress distribution can be better understood if they are interpreted graphically. Figure 4 gives the graphical representation for the displacement and stress distribution as a function of time for various distances along the length of the rod.

Theoretically, since damping is neglected, the maximum amplitudes of the motion response and stress wave will remain constant with time; however, because damping actually exists in the system the peak stresses decay with time. The higher modes of vibration generally disappear rapidly and the fundamental mode persists for a longer period of time (11, p. 37-5).

The fundamental frequency of vibration of the tensile rod was found to be 1570 cycles per second, and the calculations leading to this result can be found in the Appendix.

Response of Load Cell

Assuming that the load cell is also a fixed - free rod and following the theoretical analysis developed for the tensile rod, the fundamental frequency of vibration of the load cell was calculated to be 5940 cycles per second.
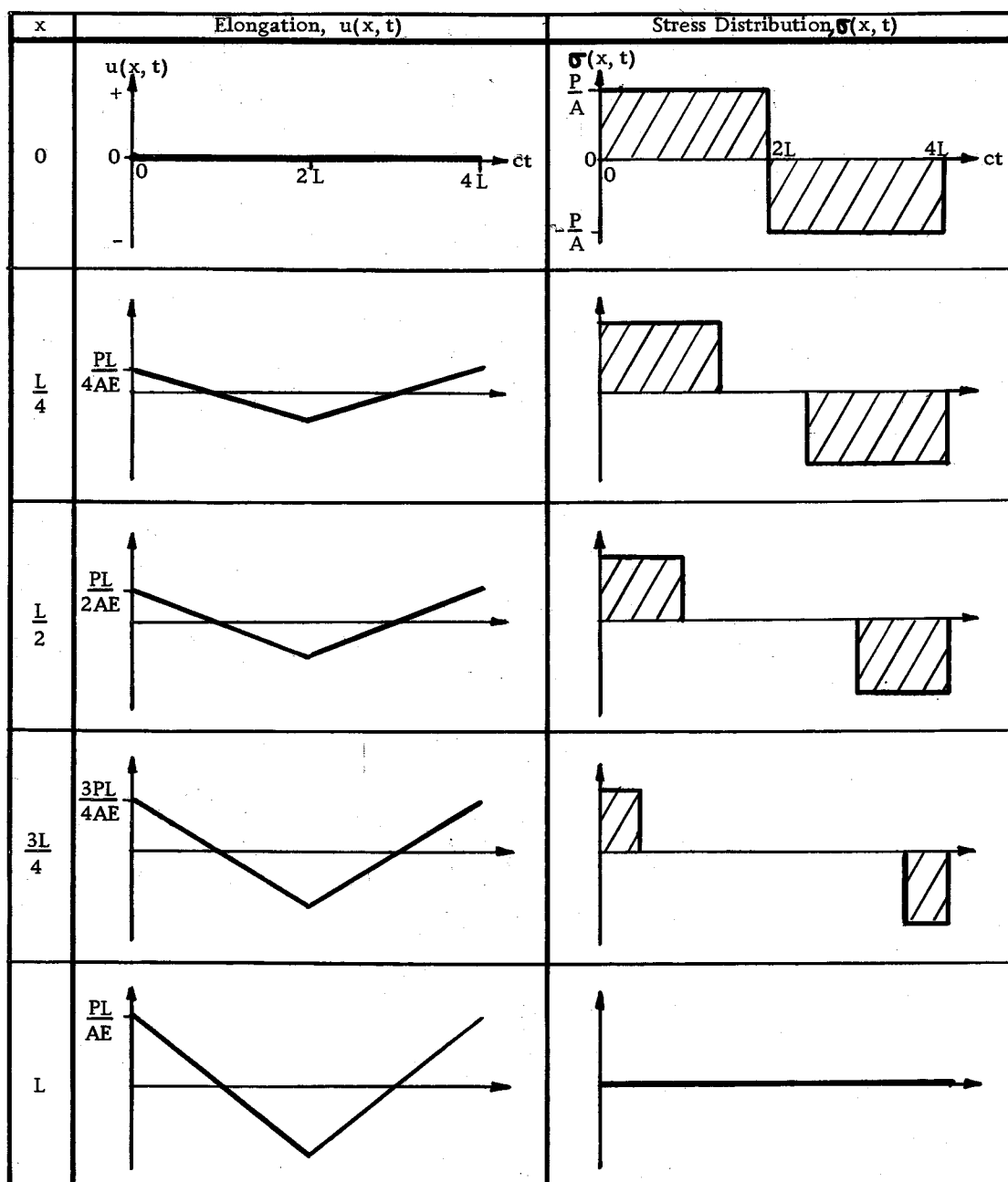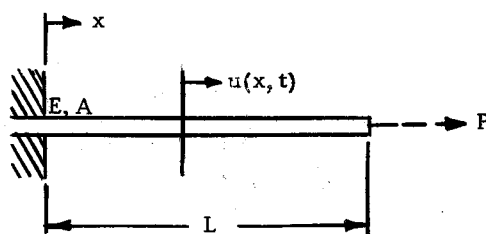
Figure 4.   Displacements and stress distributions for fixed-free rod

EXPERIMENTAL STUDIES - PART ONE

The theoretical analysis developed for the response of the system is, at best, a good approximation of the actual conditions seen by the system since the theory has been based on assumptions involving an idealized system. It has, however, supported the original supposition that peak shock loads caused by rapid stress reversals do exist. Therefore, an experimental study of the actual system response to shock loading conditions was initiated to verify the existence of the problem and to improve upon the results of the theoretical analysis, enabling a better design to be made for an energy dissipating device.

Experimental Setup

The author built and completed the cryogenic tensile testing machine described in the introduction. This testing machine was used to initiate the shock loading conditions present upon the fracturing of a tensile specimen. Gray cast iron tensile specimens were used to insure brittle fracture and notches were machined in the specimens so that fracture occurred in the loading range of 3000 to 4000 pounds. This range of maximum loading was selected so that adequate protection would be afforded the load cell against possible damage from peak stress reversals.

Two SR-4 strain gages, type A-18 having a one-eighth inch gage length, were attached three inches from the upper end of the tensile rod and one inch above the load cell on the adapter between the jack and the load cell. These gages were used to determine the strain reversals below and above the load cell. The strain gages mounted on the strain member of the load cell form a complete bridge circuit and were used to obtain a direct reading of the response of the load cell.

The change in output voltage in each gage, as a strain wave passed its position in the loading column, was displayed on the screen of a cathode ray oscilloscope after being suitably amplified. A functional diagram of the measuring equipment is shown in Figure 5.

Shielded leads were used to connect the strain gages to an Ellis strain gage amplifier, model BAM-1. The SR-4, A-18, strain gages were connected to the two arm bridge input terminals and a 120 ohm compensating resistance box was used. Since the load cell is a complete bridge circuit it was connected to the four arm bridge terminals and no compensating resistance was needed.

The output of the bridge amplifier was connected to the input of a Tektronix 535 oscilloscope having a 53-D differential high gain DC preamplifier. The unbroken test specimen was placed in series with
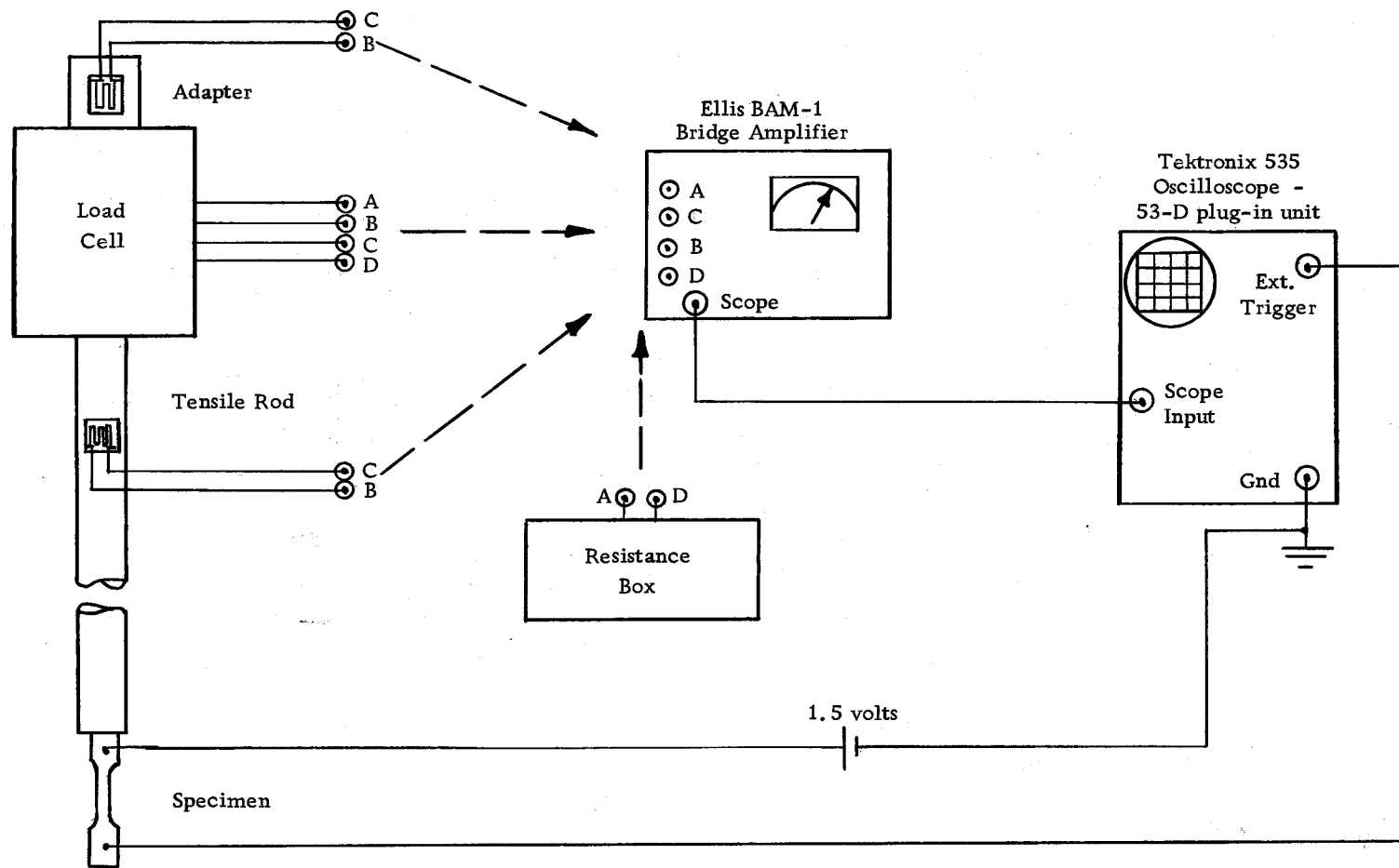
Figure 5. Circuit diagram for measuring apparatus

a 1.5 volt telephone battery forming a triggering circuit for the oscilloscope. The fracturing of the specimen broke the circuit, triggering a single sweep on the oscilloscope screen. A Fairchild - Poloroid oscilloscope camera was used to record the response curves.

When a test was run the specimen was placed in the loading column, force was applied through the jackscrew, and the specimen was fractured. The camera shutter was opened as the load was applied and closed immediately after fracture.

Only one gage at a time could be connected to the bridge amplifier because both the oscilloscope and amplifier were capable of transmitting only one signal. Thus, in order to get a complete picture of the response of the loading column, three separate tests had to be run. Because the specimens did not all break at the same load, the maximum amplitude differs with each test. This is a point which should be kept in mind when the records of the various tests are examined.

The results are essentially strain verses time curves; however, prior to actual testing, the strain readings were calibrated so that the vertical scale on the oscilloscope graticule read 1000 pounds of load per centimeter. Since each strain gage has its own gage factor

and sensitivity the calibration factor for strain-to-force transformation varied with each gage.

Results

The results of the experimental study are shown in Figures 6 through 8. Figure 6 shows the response of the tensile rod to the fracturing of the specimen. This curve is typical of shock motion. The fundamental frequency can be seen with several higher frequencies superimposed upon it. The fundamental frequency calculated from this photograph was 1080 cycles per second while the theoretical fundamental frequency was found to be 1570 cycles per second. The actual frequency is thus 68.8 percent of the theoretical frequency.

From an energy consideration it is known that the strain energy varies with the square of the applied load (10, p. 232). The equation of this relationship is:

$$\text{Strain energy} = \frac{P^2 L}{2AE}$$

By measuring the amplitudes of successive peak loads in Figure 6, and by using the above formula relating strain energy to applied load, the approximate percent of strain energy lost per cycle of vibration can be determined. The experimental data for the tensile rod shows that an average of 66 percent of the strain energy remaining in the rod was lost per cycle.
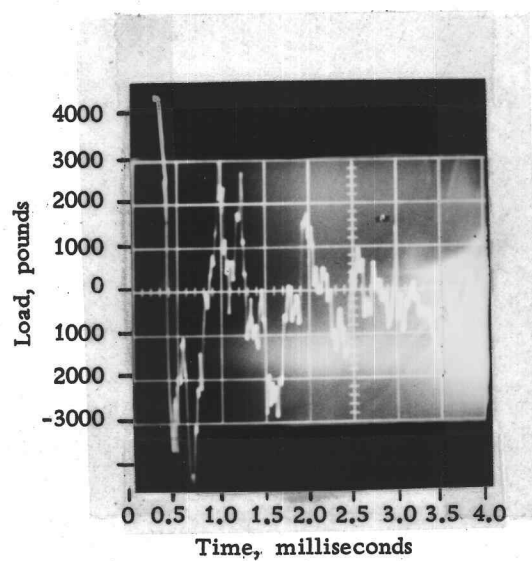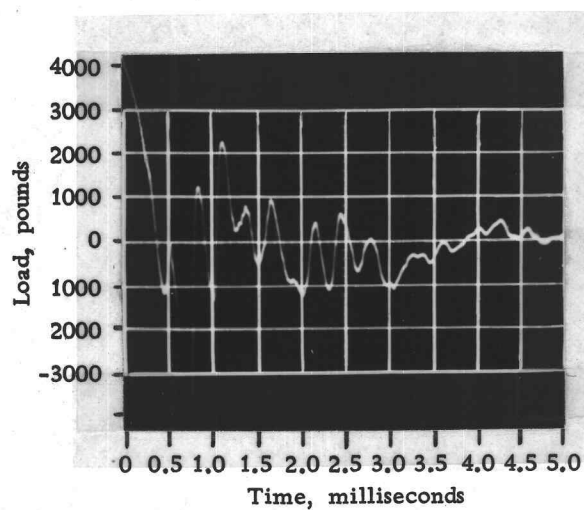
Figure 6. Response of tensile rod
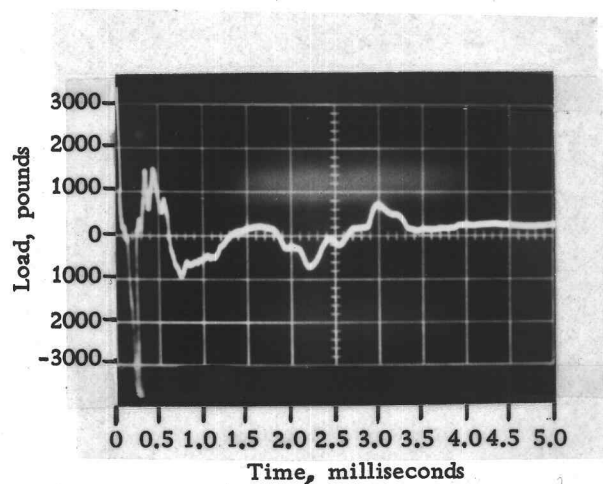

Figure 7. Response of load cell

Figure 8. Response of adapter above load cell

The response of the load cell to the shock motion of the tensile rod can be seen in Figure 7. This curve is a typical response to the type of shock environment seen in Figure 6. The fundamental frequency is the same as that found for the tensile rod, and higher vibration frequencies can be seen superimposed on it. The one higher mode that can be easily distinguished occurs at a frequency of 3250 cycles per second, and since this mode persists for a relatively long period of time it can be assumed to be the fundamental frequency of the load cell.

Figure 8 is the response of the adapter above the load cell to shock loading conditions. One peak stress reversal occurs one milli-second after specimen fracture. Two other stress reversals occur at three and nine milliseconds respectively after fracture.

Discussion

The actual boundary conditions for both the tensile rod and load cell lie somewhere between the fixed - free boundary conditions of the idealized theoretical analysis and the boundary conditions of a free - free rod. The introduction of additional constraints into a system, such as replacing the free end of a rod with a fixed end, will raise all the natural frequencies of the system (22, p. 292). Thus, the natural frequencies of the actual system should be lower than those

obtained theoretically, and the experimentally determined funda-

mental frequencies of 1080 cycles per second for the tensile rod and

3250 cycles per second for the load cell may be considered as a good

check on the respective theoretical fundamental frequencies of 1570

and 5940 cycles per second.

The first stress reversal in the load cell resulted in a com-

pressive stress almost as great as the original tensile stress; how-

ever, subsequent stress reversals yielded much lower peak stress

levels. The experimental data shows that material damping in the

system is apparently an important part of the response characteris-

tics of the load cell. After a time elapse of four milliseconds, al-

though stress reversals continue to occur, they are reduced to such

an extent that they can be considered insignificant.

Perhaps the most important result obtained from the response

curve of the load cell is the fact that rapid stress reversals do occur,

substantiating the assumed problem upon which the thesis is based.

The major stress reversals in the adapter that occur three mil-

liseconds and nine milliseconds after specimen fracture give an indi-

cation that some of the strain energy given up by the tensile rod is

transferred to the structural components of the testing machine.

These components apparently become excited in their natural fre-

quencies and, together with the inertia effects of the loading column,

induce a strain on the adapter as shown in Figure 8.

The strain gages were mounted on the surfaces of the tensile rod, load cell, and adapter; therefore, the alternate contractions and expansions in the lateral direction, resulting from Poisson's effect, are a contributing factor to the response characteristics of the system (19, p. 33).

DESIGN OF ENERGY ABSORBER

Methods of Absorbing Shock

There are basically three methods of reducing the response of a component to shock (11, p. 1-3):

1. The natural frequency of the component can be altered to eliminate resonance.

2. An auxilliary mass can be attached to the system by a spring in such a way that the vibration of the system is reduced.

3. The energy in the system can be dissipated through some external or internal means.

Of these three methods, energy dissipation is the most convenient to apply to the problem of protecting the load cell. The strain energy in the system can be dissipated by placing a shock absorber in the loading column and by using the structural damping characteristics of the testing machine.

Shock Absorbers

Shock absorbers are used to cushion the forces of velocity transition of a moving object, usually from an initial velocity to zero velocity. Since all moving masses possess energy some means must be employed to transfer this energy elsewhere when the given mass is brought to a stop. Shock absorbers accomplish this energy

transfer by absorbing the energy themselves or by transferring it to some other mechanism.

Shock absorbers may be classified as either regenerative or non-regenerative devices (7, p. 177). In regenerative shock absorbers the energy is immediately transferred back to the load in the form of "spring-back" or "bounce". Frictional forces within these devices control the amount of energy reversal and allow them to be used successfully for most cushioning applications. Examples of regenerative absorbers include solid springs, elastomers, and compressible fluids. They are relatively simple to fabricate, inexpensive, easy to apply and maintain, and generally have a long life; however, they do have spring-back and their stopping motion is non-uniform so that the stopping force increases as the stopping distance nears its maximum.

Non-regenerative shock absorbers transfer the energy of the moving load during the stopping stroke into thermal energy. Thus, if the absorber is correctly designed, the mass is left motionless at the end of the stroke. Typical examples of non-regenerative shock absorbers include frictional devices, and constant and variable orifice dampers--commonly known as dashpots. These energy dissipators are advantageous when any motion reversal or spring-back is detrimental to the system. The variable orifice damper provides

the best possible means of cushioning moving loads that are brought to rest. Its fabrication, however, can be quite complex.

Material Damping

Another mode of energy dissipation is material, or structural, damping which refers to the energy dissipation properties of materials or systems under cyclic stress but excludes energy transfer devices such as shock absorbers (14, p. 2). Generally, the problem of energy dissipation in engineering materials and structures can be solved only in an approximate, simplified form since the exact mode of damping in any specific case usually is not understood. Practical considerations dictate the use of damping terms chosen so that the governing equations of motion can be solved. It is assumed, with justification in most cases, that the solution thus obtained is a good approximation to physical reality.

Damping in any material usually can be classified as one or more of the following: viscous, coulomb, air, hysteresis, complex, negative, relaxation, magnetic, and slip. A detailed explanation of these damping modes can be found in Table 1.

In all real vibrating systems a combination of at least two types of damping will exist. Frequently, however, only one mode is predominant and the analysis can be based on that mode. Frequency

Table 1. Classification and Explanation of Damping Modes (14, p. 2)

(a)	Viscous	Damping force varies as velocity. Characteristic of low velocity motion in a high viscosity fluid: dashpots, shock absorbers.
(b)	Coulomb	Damping force is kinetic frictional force. Characteristic of dry sliding surfaces: brakes, clutches.
(c)	Air	Damping force varies as square of velocity. Characteristic of high velocity motion in low viscosity fluid: body in turbulent air at less than 0.6 Mach.
(d)	Hysteresis	Damping energy varies as function of maximum stress, usually a power function. Energy loss results from internal friction in solid bodies.
(e)	Complex	Damping force is proportional to displacement and in phase with velocity. Included as complex stiffness coefficient. An artifice to cover all cases of small damping.
(f)	Negative	Damping force feeds energy into system. Always results in system instability: oscillator with positive feedback.
(g)	Relaxation	Damping force with both positive and negative characteristics. Results in the existence of a limit cycle: Prony brake, multivibrators.
(h)	Magnetic	Hysteresis energy loss varies as the product of frequency and maximum flux density to 1.6 power. Eddy current energy loss varies as the product of frequency squared and the maximum flux density squared. Used for damping of servo motors and electrical measuring instruments.
(i)	Slip	Essentially Coulomb damping except that slip distribution gives an energy dissipation which does not, in general, vary as the first power of the amplitude of motion: built-up structures, joints.

response characteristics for a system having viscous or Coulomb

damping can be obtained without much difficulty. Systems having

other forms of damping, on the other hand, are extremely difficult

to analyze even if the exact damping expression is known.

It is well known that in practical cases the damping must be

fairly small and the motion nearly sinusoidal in order to make use

of approximations necessary to solve the problem (14, p. 7). In

these cases the behavior of the theoretical system will often follow

closely that of the actual system. If these approximations for damp-

ing cannot be determined or if a reasonable choice of damping terms

leads to an unmanageable equation of motion, then the emperically

derived expressions for energy loss per cycle or the actual stress-

strain curves for the material must be used.

Since in all practical applications damping is one of the more

elusive variables that a designer must use, it is important that the

extent of the damping approximations be thoroughly investigated for

each case.

Requirements and Selection of Absorber

The ideal shock absorber, for adequate reduction of peak

stress reversals in the load cell, should meet the following require-

ments:

1. A large quantity of mechanical energy should be absorbed within a short period of time.

2. The force transmitted to the load cell should be much smaller in magnitude than the maximum force exerted on the system just prior to specimen fracture.

3. A large part of the material's stress-strain curve should contain a constant stress.

4. The energy released by the shock absorber must not be detrimental to the integrity of the system.

5. The natural frequency of the absorber must be lower than that of the tensile rod so that excitation of both the load cell and tensile rod is small.

6. It must perform its functions within a limited space.

7. Its fabrication should be simple and economical.

8. It should be able to withstand repeated loading with no permanent deformation.

Many practical methods of absorbing and damping the shock loading were analyzed and their characteristics were compared with the requirements of the system as set forth in this section. After a careful study of various methods it was found that the properties of cushioning materials, such as the flexible plastic foams, corresponded closely with the system's requirements. Thus, it was decided that the energy dissipating device be designed around such a material.

All materials utilized to provide cushioning may be classified as either elastic (flexible) or inelastic (crushable). Materials placed

in the first category have a permanent deformation of not more than ten percent after compression to a 65 percent strain level (11, p. 41-13). In order to satisfy the requirements of the system, the elastic material should be used, thus eliminating the need to replace the material after each test.

The excellent compressive energy absorbing properties of a cushioning material can be employed by designing a shock absorber having a piston and cylinder arrangement with the cushioning material placed between the piston and cylinder head. Such a design for the application under consideration was first suggested by Gordon Hull (13, p. 43) and appears to be the simplest and most effective method adaptable to the system. All further analysis and design of the shock absorber will be based on this design proposal.

Among the elastic cushioning materials available that can be incorporated into the shock absorber design are the following: polyester and polyether urethane foam, polyethylene foam, latex hair, and reclaimed latex foam. Of these materials polyester urethane and polyethylene foams have the best energy absorbing properties and will be studied further.

The quantity of cushioning material required for a shock absorber can be determined by the amount of energy that must be stored and dissipated by the material. The strain energy stored in

a unit volume of the resilient material may be defined in terms of stress and strain and is equal to the area under the stress - strain curve. Since the elastic modulus varies with strain for viscoelastic materials, a graphical integration of the stress - strain curve must be used to obtain the amount of energy stored for a given strain. Compressive stress - strain diagrams for polyester and polyethylene foams are shown in Figures 9 and 10.

Design Parameters

The parameters for the shock absorber design, from both theoretical and experimental considerations of the system, are as follows:

1. Strain energy to be dissipated under maximum load - 1720 inch - pounds. (Theoretical)

2. First natural frequency of tensile rod - 1080 cycles per second. (Experimental)

3. First natural frequency of load cell - 3250 cycles per second. (Experimental)

4. Approximate reduction per cycle of strain energy in loading column when tensile rod is rigidly attached to load cell - 66 percent. (Experimental)

5. Time required for significant stress reversals to damp out - approximately 4 milliseconds. (Experimental)

As noted above, it was found that approximately 66 percent of the total energy stored at the beginning of each cycle was dissipated
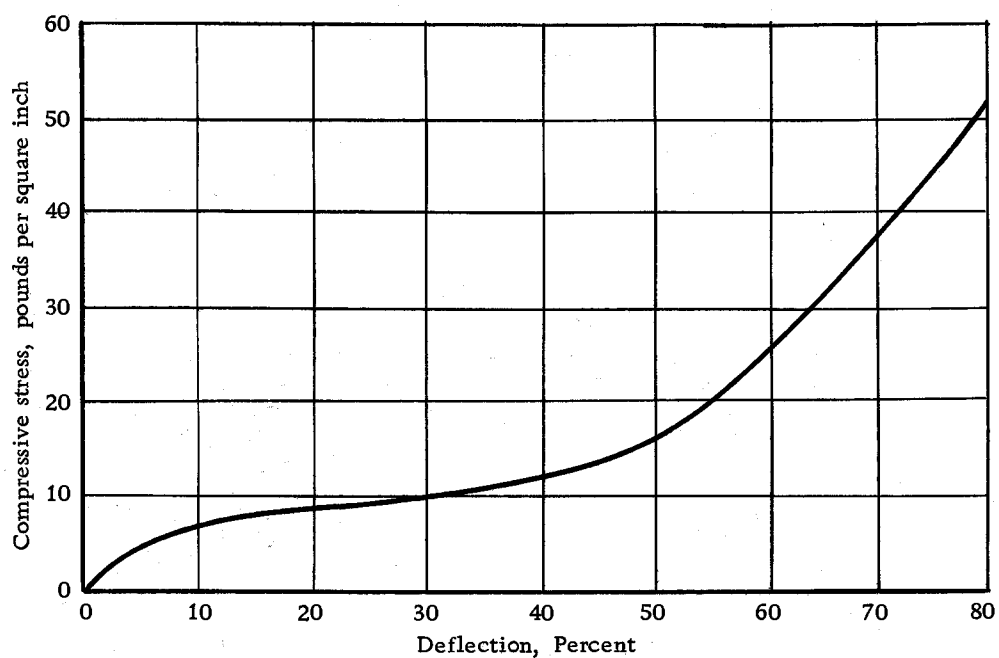
Figure 9. Compressive stress-strain curve for
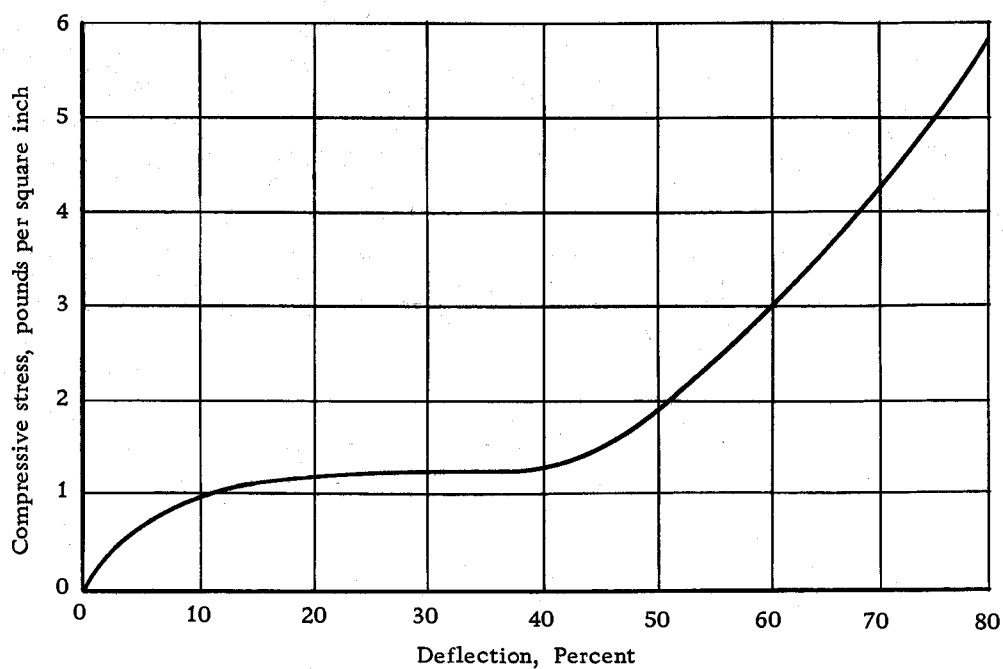polyethylene foam (6, p. 3)

Figure 10. Compressive stress-strain curve for
polyester urethane foam (11, p. 41-15)

at the end of that cycle. The maximum compressive stress of the

tensile rod is exerted on the load cell at the end of a half cycle.

Assuming that the amount of energy dissipated internally is a linear

function of the percent of a cycle completed, 33 percent of the energy

initially in the system will be dissipated in the structure by the time

the initial peak compressive stress reaches the load cell. For the

maximum loading condition of 20,000 pounds, the internal energy

dissipation at the end of the first half cycle should amount to 570 inch-

pounds, leaving 1150 inch-pounds to be dissipated either in succeed-

ing cycles or by another means. It should be noted that the basis

for this assumption is the experimental data obtained while the ten-

sile rod was rigidly attached to the load cell.

Shock Absorbant

The volume, V, of energy absorbing material needed to dissi-

pate the strain energy, W, of the system in one cycle is:

$$V = \frac{W}{U}$$

where U represents the energy capacity per unit volume of cushion-

ing material and is equal to the area under the stress - strain curve

of the material. It is desirable to absorb all of the strain energy in

the tensile rod during the first compressive stroke of the shock ab-

sorber and the preliminary design will be calculated on this basis.

The required volume of cushioning material was calculated for polyethylene and polyester urethane foams.

Polyethylene Foam

Referring to Figure 9, a deflection of 75 percent of the original thickness corresponds to a compressive stress of 46 pounds per square inch. The area under the stress - strain curve for this stress level represents 13.7 inch-pounds per cubic inch of potential absorbing energy, as measured with a planimeter.

The required volume of polyethylene foam is then:

$$V = \frac{1150 \text{ inch-pounds}}{13.7 \frac{\text{inch-pounds}}{\text{cubic inch}}} = 85 \text{ cubic inches}$$

Assuming that the foam has a circular cross-sectional area with a diameter of six inches, the required thickness of the foam must be:

$$h = \frac{V}{A} = \frac{85}{9\pi} = 3.0 \text{ inches}$$

The deflection corresponding to a 75 percent strain level for a three inch thickness is 2.25 inches.

The force transmitted to the load cell under maximum loading conditions through the polyethylene foam is:

$$P = \sigma A = (46)(28.3) = 1300 \text{ pounds}$$

The load reduction factor of the shock absorber is then:

$$T = \frac{\text{maximum force seen by load cell after specimen fracture}}{\text{maximum force exerted on system prior to specimen fracture}}$$

$$= \frac{1300}{20,000} = 0.065$$

That is, 6.5 percent of the original load is seen by the load cell upon fracture of the specimen.

A larger cross-sectional area of material would reduce the thickness of the foam, but would increase the load reduction factor. A smaller cross-sectional area would decrease the load reduction factor but would require a much greater thickness. It is felt that for the requirements of the system the polyethylene foam should be six inches in diameter and three inches thick.

Polyester Urethane Foam

Following the same procedure as for polyethylene foam, the required dimensions for the polyester urethane foam were determined.

Again using a planimeter, the area under the stress - strain curve in Figure 10 for an 80 percent strain represents 1.2 inch-pounds per cubic inch of energy absorbing capacity, a much lower value than that found for polyethylene foam. The required volume of polyester foam, from the above data, is 935 cubic inches. For a six inch diameter the thickness required would be 33.0 inches. It can be

seen that polyester foam theoretically is not a suitable shock absorbing medium for the load cell because of the great volume of material required.

Shock Absorber Assembly

As shown in Figure 11 the basic shock absorber assembly is a piston and cylinder arrangement. For ease of fabrication the cylinder was made from seamless steel tubing with flanges welded at both ends. The cylinder caps were then bolted to the flanges after insertion of the foam material and piston assembly. The piston was made of one-half inch steel plate and the piston rod was bolted to the piston.
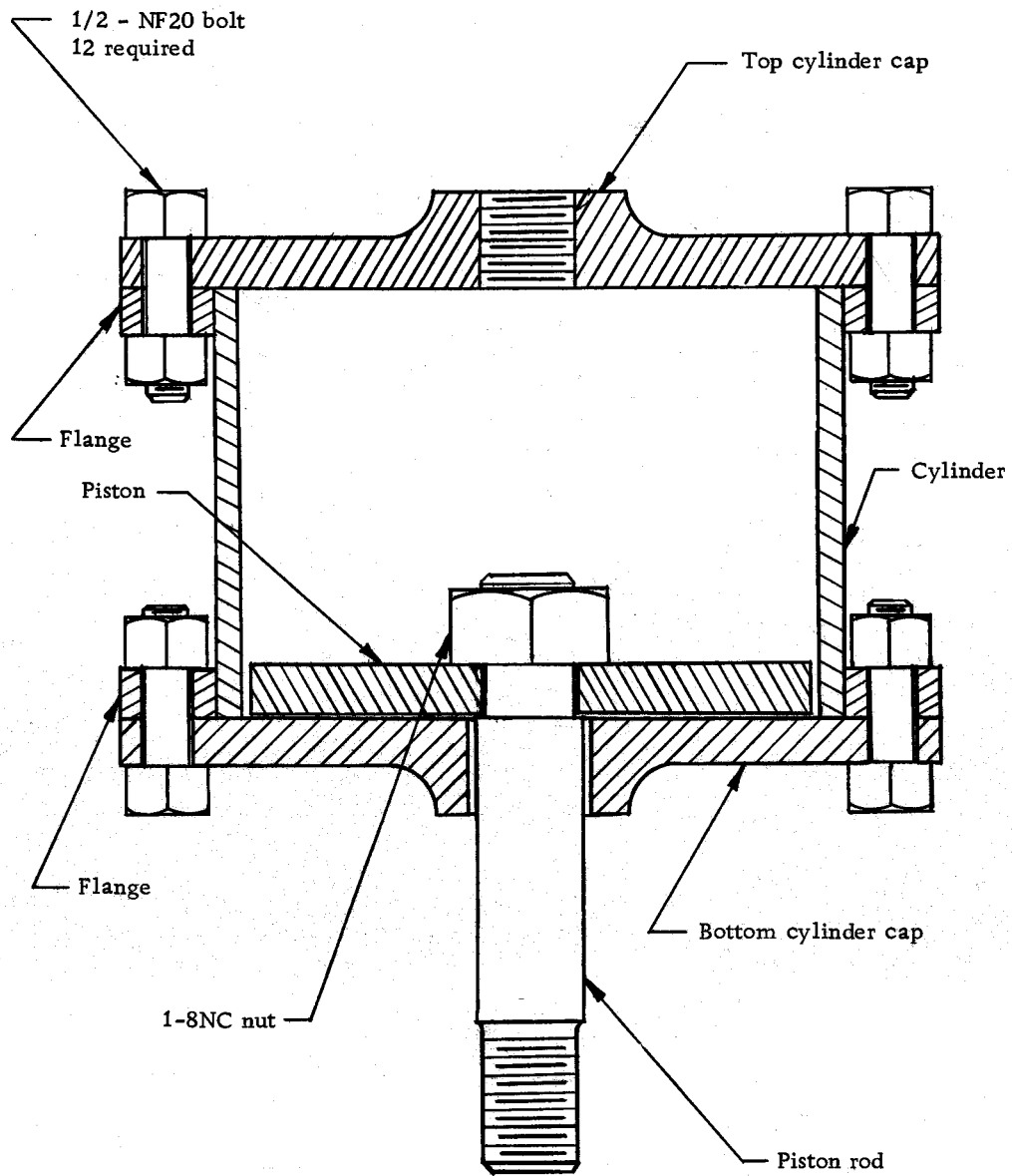
Cylinder Assembly

The cylinder was made of Shelby seamless thickwalled tubing--a cold drawn AISI 1020 steel. Its yield stress is 62,000 pounds per square inch and its tensile strength is 74,000 pounds per square inch (20, p. 495).

Using a cylinder wall thickness of a quarter inch, the cross-sectional area available for axial loading during the tensile load application is:

$$A = \frac{\pi}{4} [(6.5)^2 - (6.0)^2] = 5.03 \text{ square inches}$$

1/2 - NF20 bolt
12 required

Top cylinder cap

Flange

Piston

Cylinder

Flange

Bottom cylinder cap

1-8NC nut

Piston rod

Scale: 1/2 inch = 1 inch

Figure 11. Shock absorber assembly

The maximum stress is:

$$\sigma = \frac{P}{A} = \frac{20,000}{5.03} = 3980 \text{ pounds per square inch}$$

The design factor of safety is thus

$$D.F. = \frac{62,000}{3980} = 15.7$$

Following the procedure used by Gordon Hull for his design thesis on the cryogenic tensile testing machine (13, p. 83) the design factor of safety for the shock absorber assembly was established at 2.0. The axial stresses in the cylinder case are well within this design factor.

The flanges welded to the cylinder are one half inch thick and their outside diameter is 8.50 inches. The inside diameter of the flanges and the outside diameter of the cylinder casing is 6.50 inches.

A one-quarter inch fillet weld was used on both sides of the flanges to attach them to the cylinder casing. The approximate weld stress due to shear and bending at maximum load is (20, p. 211):

$$\sigma = \frac{P}{d\,a(b + h)} \sqrt{2 L^2 + \frac{(b + d)^2}{2}}$$

$$= \frac{20,000}{(0.25)(6.5\pi)(0.75)} \sqrt{2(0.5)^2 + \frac{(0.75)^2}{2}}$$

$$= 4620 \text{ pounds per square inch}$$

Therefore, the use of a one-quarter inch weld is acceptable, as the American Welding Society recommends a maximum stress of 13,600 pounds per square inch (18, p. 383). Detail drawings of the flanges and cylinder assembly are shown in Figures 12 and 13.

One half inch bolts were used to attach the cylinder caps to the flanges. It is advantageous to preload the bolts so that no separation will take place between the flanges and cylinder caps at maximum load. In order to prevent this separation, the preload must be at least equal to the maximum load. A 30 percent overshoot on pre-loading is recommended by Shigley (20, p. 203); therefore, a preload of 26,000 pounds is specified.

The yield strength of SAE grade 5 bolts is 85,000 pounds per square inch (20, p. 190). Using the design factor of safety, the design strength of the bolts is:
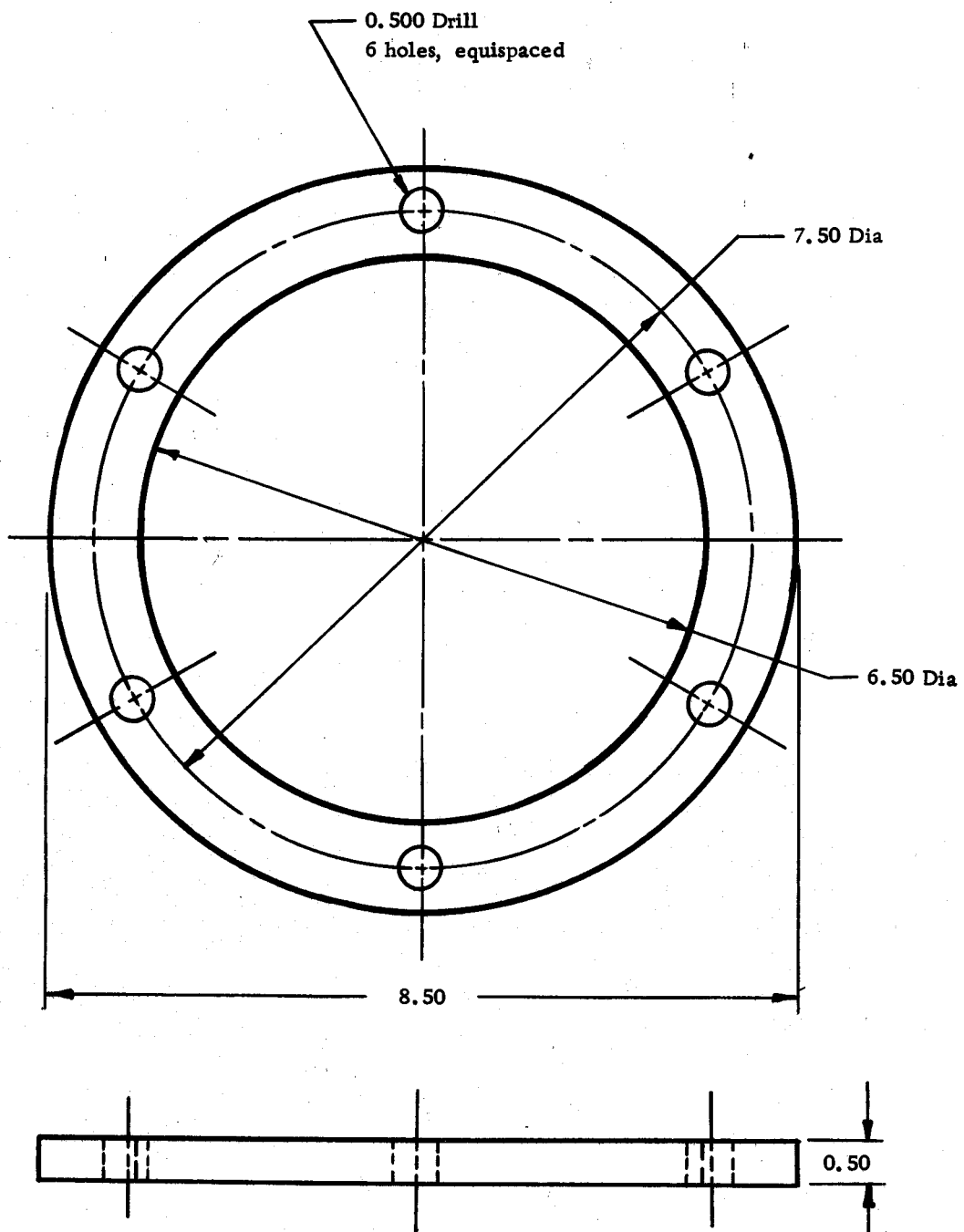
$$\text{Design strength} = \frac{85,000}{2} = 42,500 \text{ pounds per square inch}$$

The total required cross-sectional area of the bolts, under maximum load, is:

$$A = \frac{P}{\sigma} = \frac{20,000}{42,500} = 0.470 \text{ square inches}$$

The stress area for a 1/2 - 20 NF bolt is 0.1597 square inches. Therefore, the required number of bolts is:

0.500 Drill
6 holes, equispaced

7.50 Dia

6.50 Dia

8.50

0.50

Scale: 1/2 inch = 1 inch
Material: AISI 1020 mild steel
Two required

Figure 12. Flange

Flange

Cylinder
(Seamless
tubing – 1/4
inch wall
thickness)

0.50

4.50

0.50

1/4

Flange

6.00 Dia

6.50 Dia
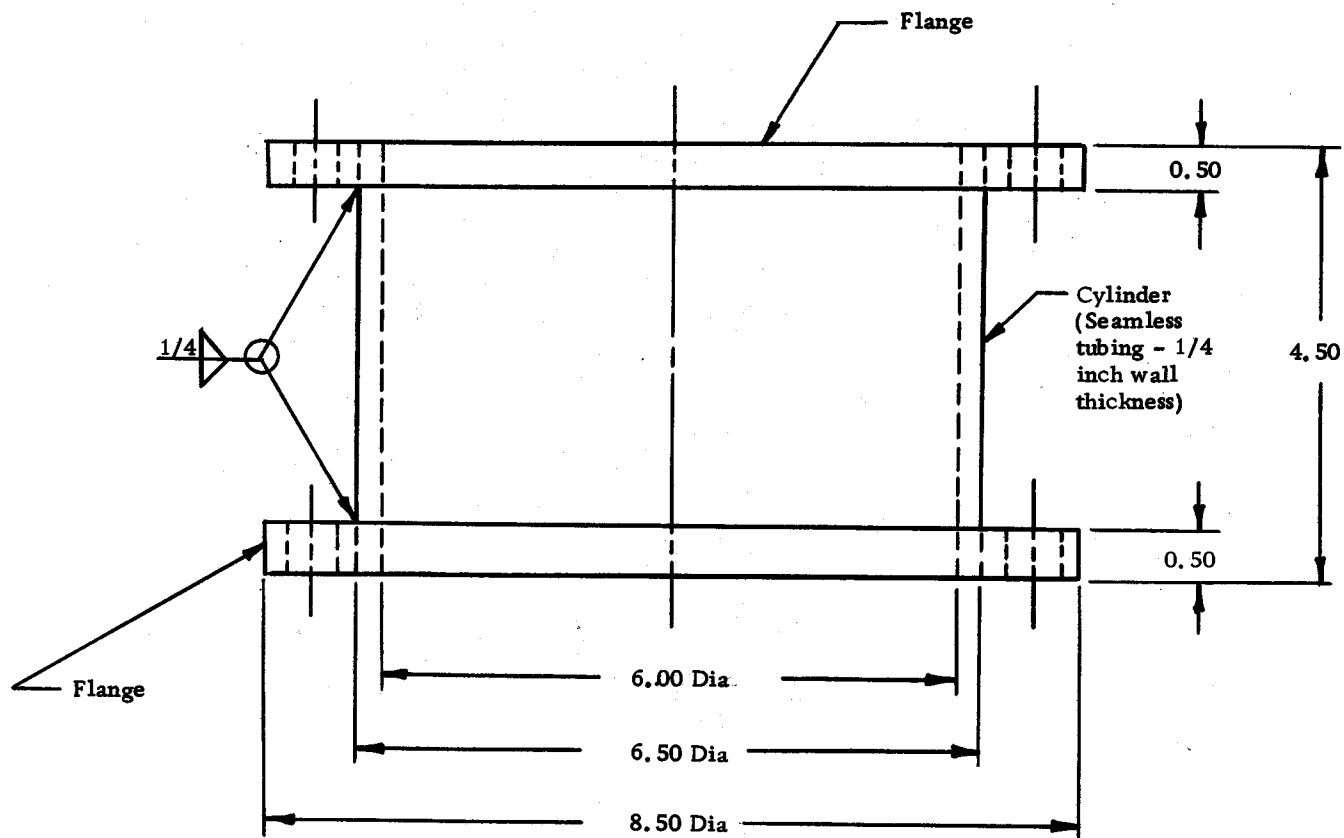
8.50 Dia

Scale: 1/2 inch = 1 inch

Figure 13. Cylinder assembly

$$N = \frac{0.470}{0.160} = 2.94 \text{ bolts}$$

Three 1/2 - 20 NF bolts are adequate in strength; however, since there is sufficient room around the flange, six bolts have been used.

The approximate torque necessary to preload each bolt is (20, p. 190):

$$M = 0.20 \text{ (force on bolt)(bolt diameter)}$$

$$= \frac{(0.20)(20,000)(0.50)}{6}$$

$$= 433 \text{ inch-pounds}$$

Figures 14 and 15 show detail drawings of the cylinder caps.

Piston Assembly

AISI 4140 cold rolled steel was used for the piston rod. Its yield strength is 90,000 pounds per square inch and its tensile strength is 102,000 pounds per square inch. The upper end of the rod is threaded and connected to the piston with a nut as shown in Figure 11.

Assume a 1 - 8 NC thread on the upper end of the piston rod. The effective shear area per inch of thread length for a 1 - 8 NC thread is 2.36 square inches (13, p. 83). For a maximum load of 20,000 pounds the shear stress in the threads, using a nut having a one inch thickness, is:
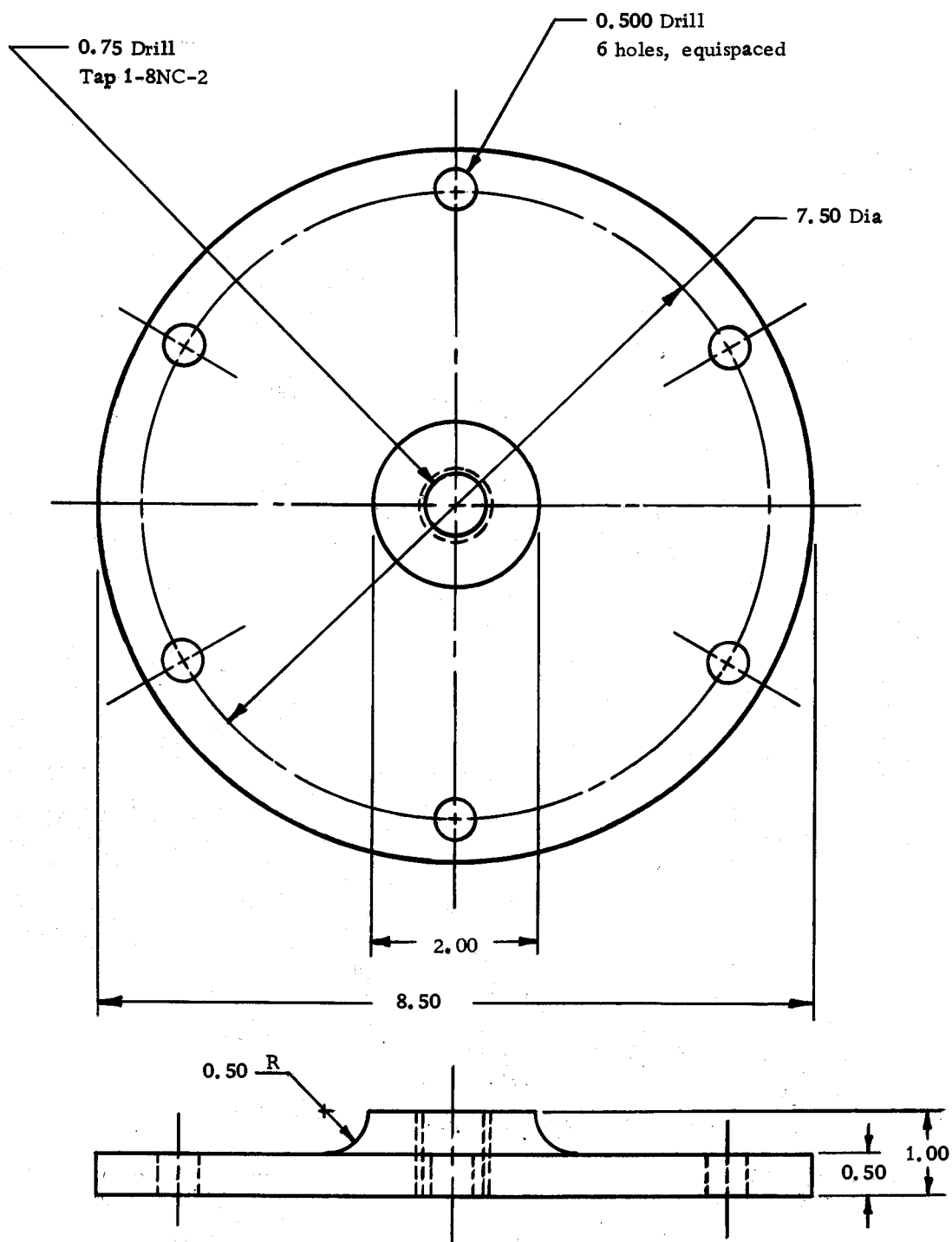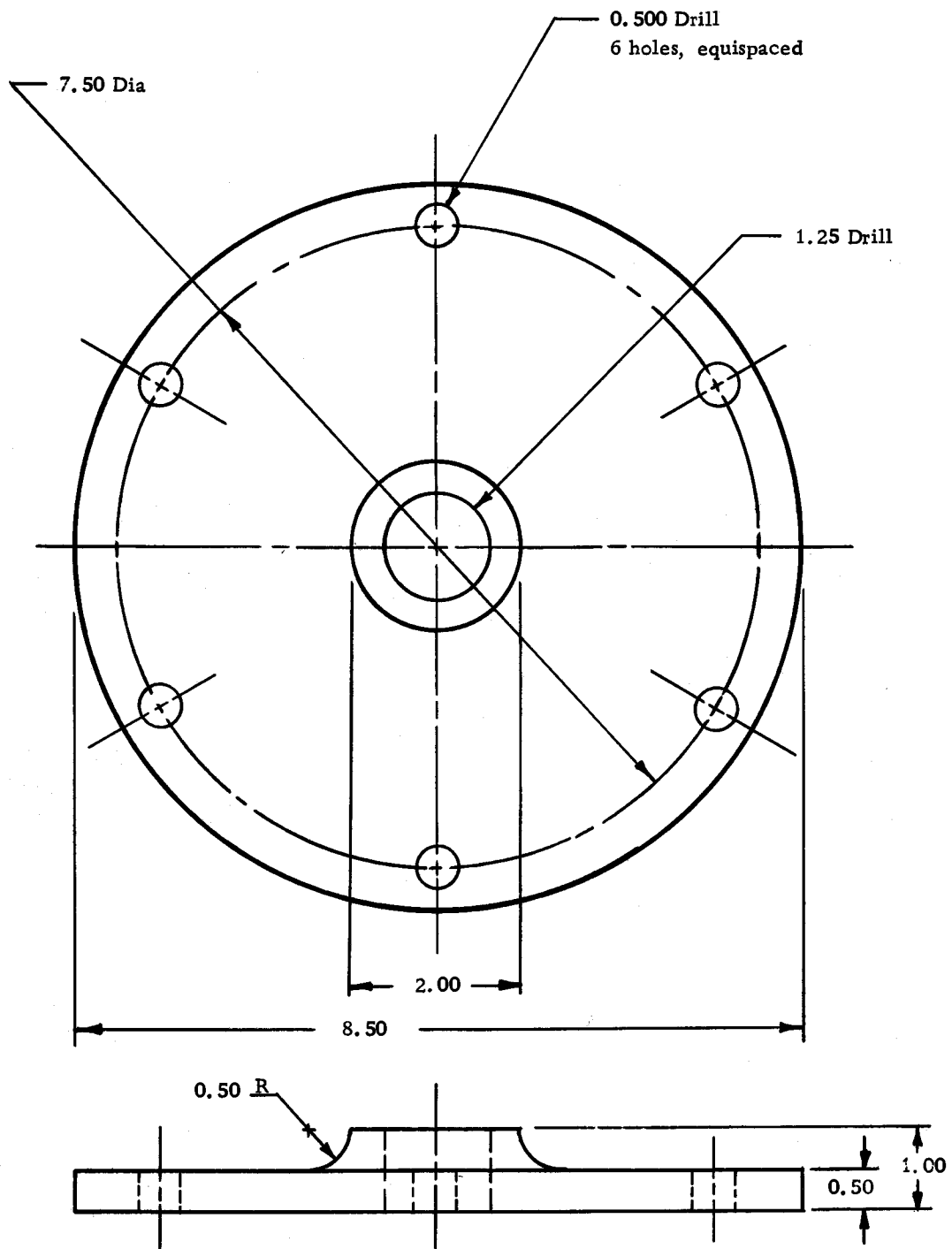
0.75 Drill
Tap 1-8NC-2

0.500 Drill
6 holes, equispaced

7.50 Dia

2.00

8.50

0.50 R

1.00

0.50

Scale: 1/2 inch = 1 inch
Material: AISI 1020 mild steel
One required

Figure 14. Top cylinder cap

0. 500 Drill
6 holes, equispaced

7. 50 Dia

1.25 Drill

2.00

8.50

0.50 R

1.00
0.50

Scale: 1/2 inch = 1 inch
Material: AISI 1020 mild steel
One required

Figure 15. Bottom cylinder cap

$$\sigma_s = \frac{P}{A} = \frac{20,000}{2.36} = 8500 \text{ pounds per square inch}$$

The axial tensile stress in the piston rod is highest at the threads.
The effective stress area for a 1 - 8 NC thread is 0.5510 square
inches (13, p. 83). The maximum tensile stress in the rod is then:

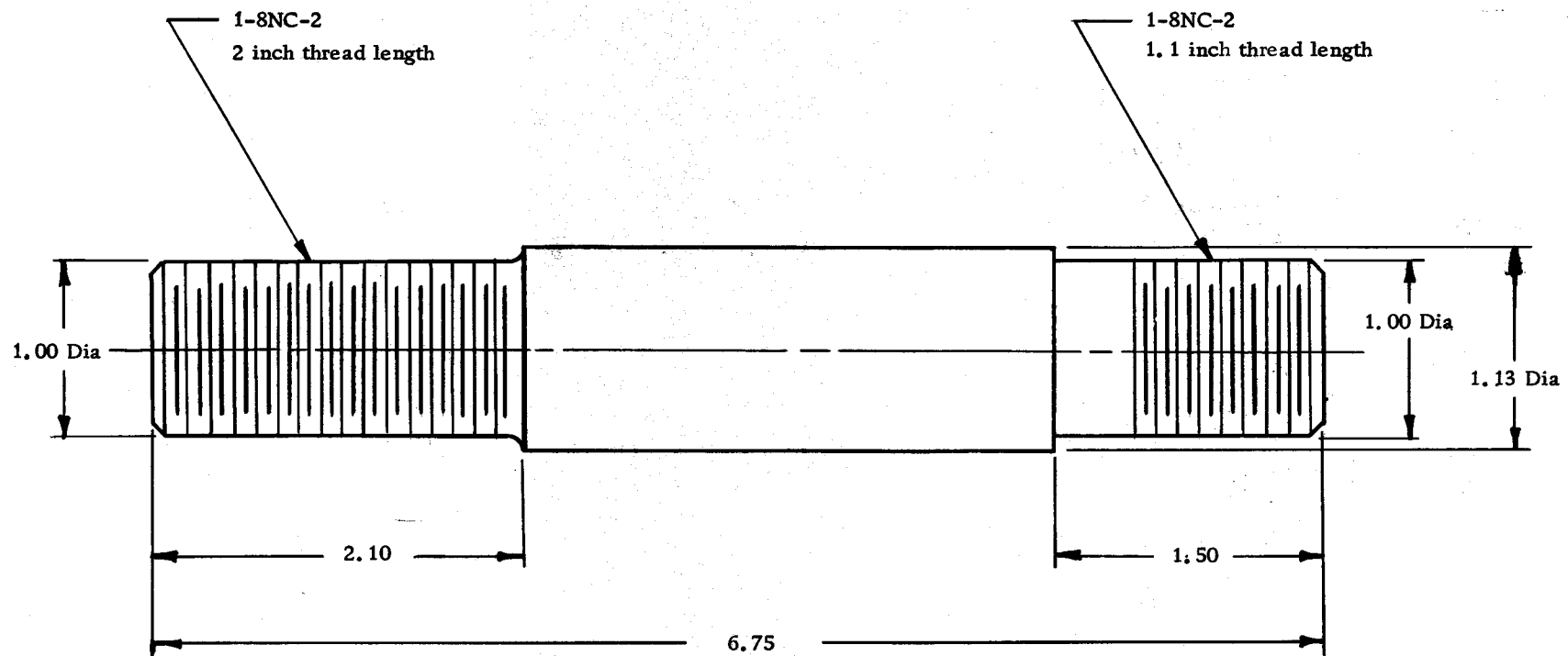$$\sigma = \frac{P}{A} = \frac{20,000}{0.5510} = 36,200 \text{ pounds per square inch}$$

The design factor based on this tensile stress is:

$$\text{D.F.} = \frac{90,000}{36,200} = 2.48$$

which is acceptable.

The lower end of the piston rod also has 1 - 8 NC threads so
that it can be connected to the tensile rod through an adapter already
in existence. Figures 16 and 17 are detail drawings of the piston
rod and piston.

Since the piston assembly contains a one inch nut on top of the
piston, the thickness of foam must be increased from three to four
inches so that the nut will not bottom out on the top cylinder cap.
The additional thickness of polyethylene foam increases the volume
from 85 cubic inches to 113 cubic inches. The strain energy per
cubic inch that must be absorbed by the foam is now reduced from
13.7 inch-pounds per cubic inch to 9.9 inch-pounds per cubic inch.
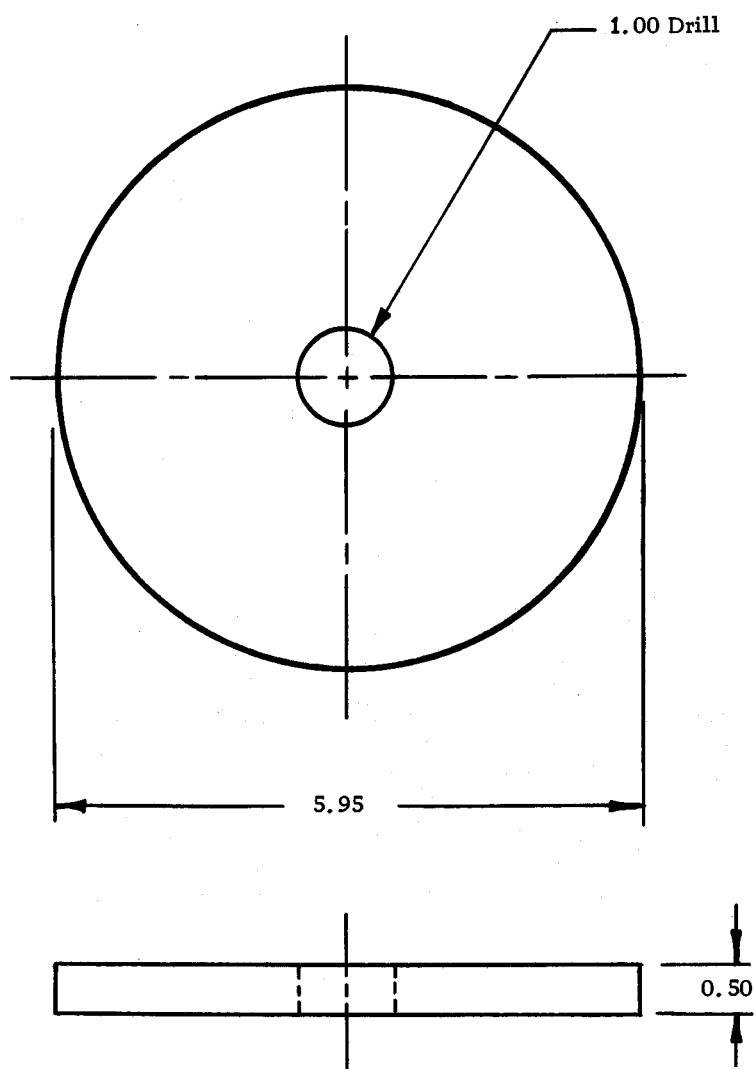From Figure 9 the corresponding stress level is 34 pounds per

1-8NC-2
2 inch thread length

1-8NC-2
1. 1 inch thread length

1.00 Dia

1.00 Dia

1.13 Dia

2.10

1.50

6.75

Scale: 1 inch = 1 inch
Material: AISI 4140 cold rolled steel
One required

Figure 16.   Piston rod

1.00 Drill

5.95

0.50

Scale: 1/2 inch = 1 inch
Material: AISI 1020 mild steel
One required

Figure 17. Piston

square inch and the strain becomes 0.67 inches per inch. The force

transmitted to the load cell is reduced to:

$$P = (34)(28.3) = 965 \text{ pounds}$$

The load reduction factor of the shock absorber becomes:

$$T = \frac{965}{20,000} = 0.048$$

The maximum deflection corresponding to a 67 percent strain level

is 2.58 inches. Therefore, theoretically, the piston assembly will

not bottom out on the top cylinder cap.

The primary reason for increasing the foam thickness rather

than decreasing the thickness of the nut protruding above the piston

is that it may be desirable to have a larger volume available within

the cylinder when further testing is done on the shock absorber.

Figure 18 is a photograph of the shock absorber mounted in the

testing machine. The Baldwin U-1 load cell can be seen directly

above the shock absorber. Figure 19 shows the disassembled shock
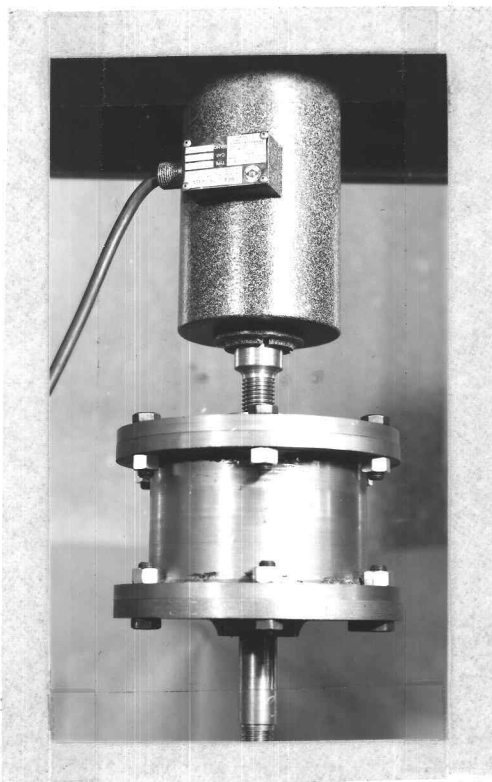
absorber assembly.

Figure 18. Closeup of shock absorber and
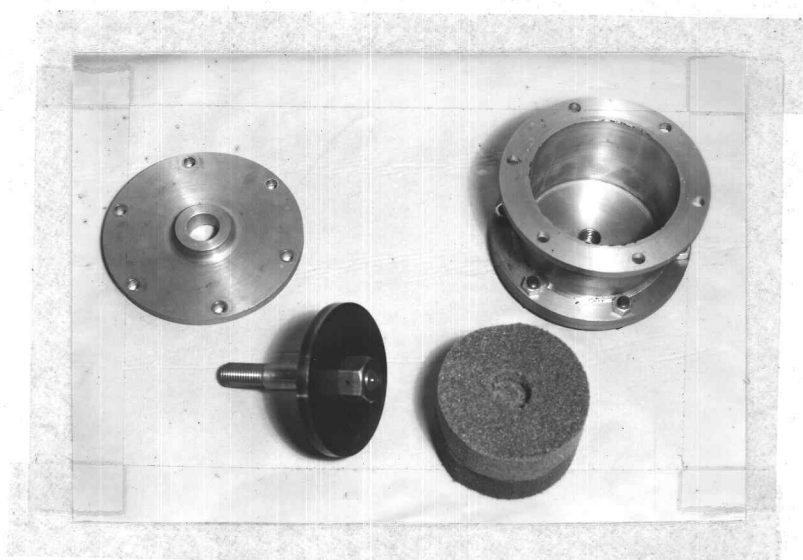load cell as mounted in testing
machine

Figure 19. .Shock absorber disassembled

EXPERIMENTAL STUDIES - PART TWO

Experimental Setup

After fabrication of the shock absorber it was necessary to test it so that its actual effectiveness could be determined. The testing procedure previously used was followed except that the shock absorber was placed between the load cell and the tensile rod, as shown in Figure 20 and response curves were made only for the load cell. The tensile specimens were machined so that they fractured at approximately 3000 pounds of load. Tests were run using polyethylene and polyester urethane foams as the cushioning materials.

Results

Figure 21 shows the response curve for the load cell with polyethylene as the absorbing medium. The initial load release after fracture is adequately damped; however, three milliseconds after fracture a peak compressive stress is seen by the load cell. The small oscillations seen occurred at 3250 cycles per second and correspond with the results of the load cell response found in the initial experimental studies.

Figure 22 gives the response of the load cell when polyester foam was used. A peak compressive stress similar to the one in
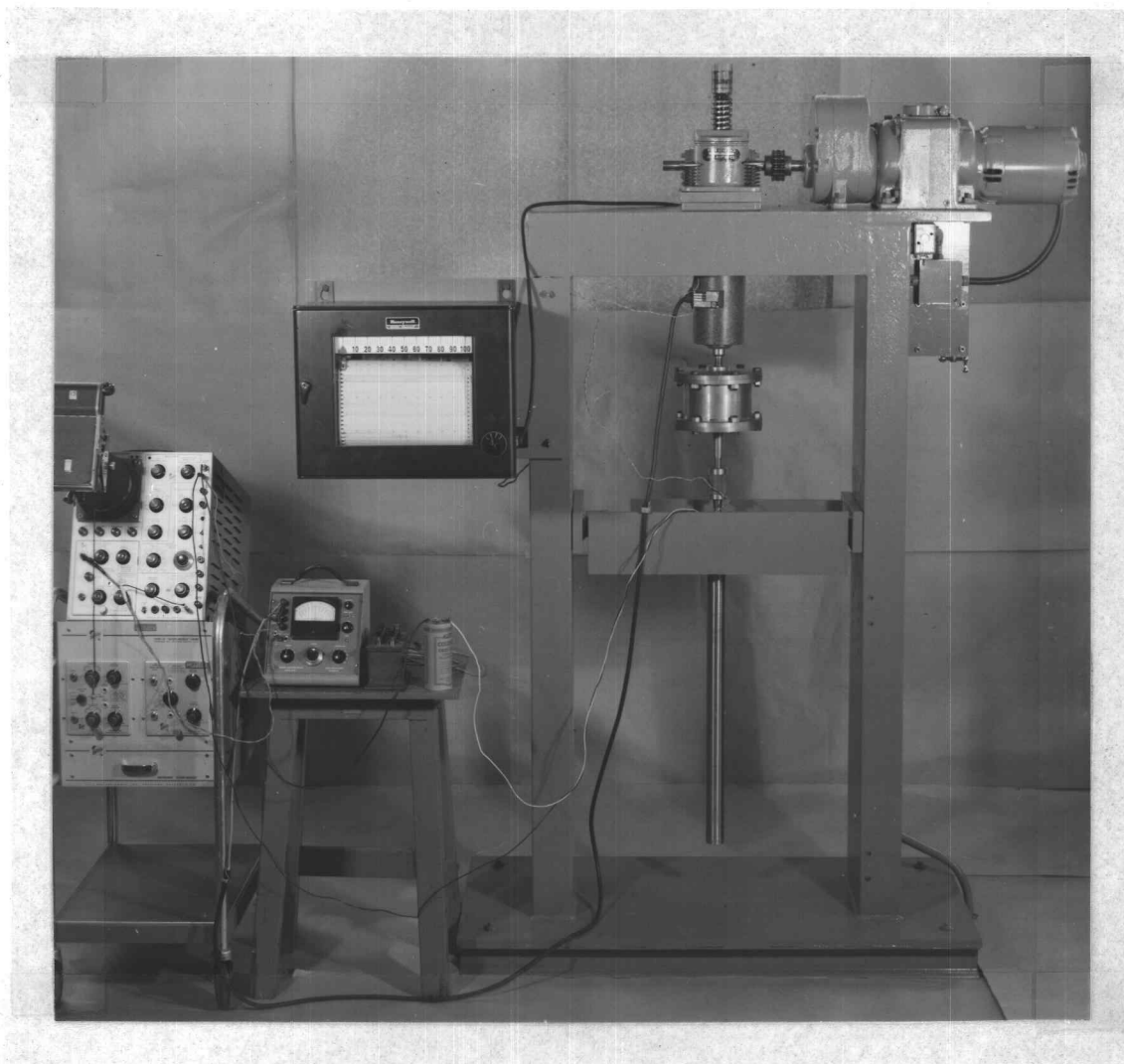
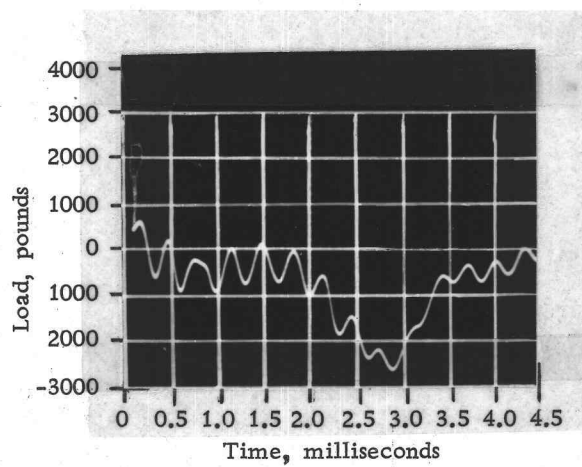Figure 20. Experimental setup with shock absorber

Figure 21. Response of load cell using
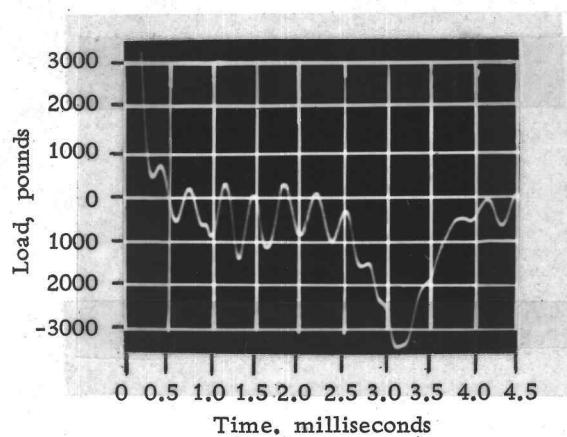polyethylene as shock ab-
sorbing medium

Figure 22. Response of load cell using polyester
urethane as shock absorbing medium

Figure 21 can once again be seen. Since the peak compressive stress found in both tests seem to be consistant both in magnitude and in time, it was decided that the cause of these stresses was external to the shock absorber.

The apparent explanation for the existence of this peak compressive stress involves the motion of the top plate of the testing machine after the specimen fractures. It was theorized that the strain energy initially present in the load cell and jack screw is transmitted to the top plate and surrounding structure upon specimen fracture. This additional strain energy in the top plate, together with the response of the top plate and the inertia effects of the load cell and jack screw, cause the peak compressive stress to be seen by the load cell three milliseconds after the load is released.

One means of eliminating this peak compressive stress is to place another shock absorber between the load cell and the jack; however, limited space in the loading column prohibits the use of this solution.

Another solution to the problem would involve spring mounting the jack to the top plate. Then, when the top plate responds to the sudden load release, the jack and load cell would not be rigidly attached and the peak compressive stress on the load cell should be greatly reduced.

To establish the validity of this explanation of and solution to the problem, springs having a stiffness coefficient of 60 pounds per inch were placed between the top of the jack mounting plate and the heads of the bolts attaching the jack to the top plate. This arrangement can be seen in Figure 20.

A test was then run using polyethylene foam and Figure 23, shows the response of the load cell with the jack spring mounted to the top plate. The specimen broke at about 4000 pounds and the maximum compressive load was 600 pounds. This maximum compression also occurred three milliseconds after fracture and was most likely due to the response of the top plate. The maximum load reduction factor for this test was:

$$T = \frac{600}{4,000} = 0.150$$

Figure 24 shows the response of the load cell using polyester foam in the shock absorber in conjunction with the spring mounted jack. The large stress reversals are an indication that the polyester foam bottomed out.

Discussion

The results of the tests made on the system that included the polyethylene foam in the shock absorber in conjunction with the
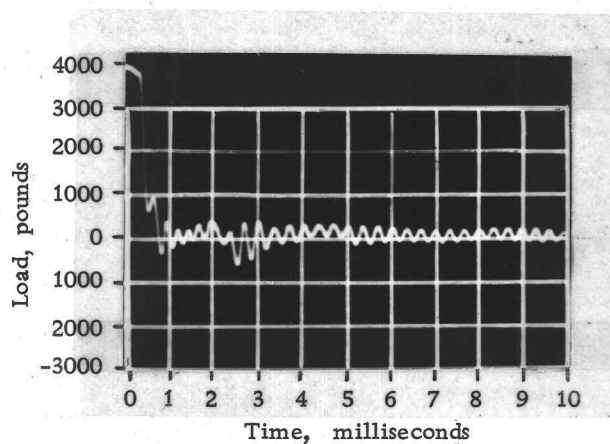
Figure 23. Response of load cell using polyethylene in shock absorber and spring mounts on the jack
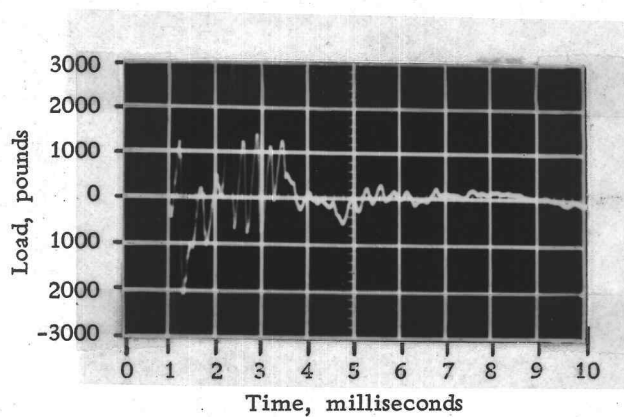

Figure 24. Response of load cell using polyester urethane in shock absorber and spring mounts on the jack

spring mounted jack shows that the strain energy in the system was adequately dissipated and the load cell saw relatively small stress reversals. The maximum load reduction factor was 0.150. For an initial load of 4000 pounds design calculations predict a maximum load reduction factor of 0.03 and a maximum load of 117 pounds being imparted on the load cell. The experimental results indicate that the motion of the top plate increases the magnitude of the stress rever- sals seen by the load cell after specimen fracture, accounting for the higher load reduction factor. If the response curve for the load cell in Figure 23 is carefully studied, the load reversals present after the influence of the top plate has subsided have a maximum amplitude of 200 pounds. The corresponding load reduction factor of 0.050 is in satisfactory agreement with the theoretical load re- duction factor of 0.03 if the effect of the top plate on the response of the load cell is neglected.

The results of the test using the polyester foam as the shock absorbing medium in combination with the spring mounted jack pre- sented evidence that the polyester foam is inadequate in absorbing the strain energy in the system for loading conditions as small as 3000 pounds.

The fact that the frequency which persisted in the load cell for

all tests performed occurred at 3250 cycles per second, as shown in

Figures 21 through 24, further substantiates the conclusion previous-

ly reached that the fundamental frequency of the load cell is 3250

cycles per second.

CONCLUSIONS

1. The supposition that peak stress reversals occur in the load cell upon specimen fracture was verified by experimental evidence.

2. The fact that peak stress reversals actually damage the load cell has not been proven or disproven although, as noted in the intro- duction, previous experience indicates that such damage does occur.

3. The initial assumption that the top plate could be considered as a rigid body was proven to be in error.

4. The theoretical natural frequencies of the tensile rod and load cell are in satisfactory agreement with those found experimen- tally.

5. Polyethylene and polyester urethane foams were found to be effec- tive energy absorbers under a shock environment. For the prob- lem under consideration, however, only polyethylene foam proved to be a practical and satisfactory solution.

6. The addition of spring mounts on the jack solved the problem of a peak compressive stress being induced on the load cell three milliseconds after the strain energy in the system was released.

7. The design of the shock absorber was found to be adequate and

was relatively simple to fabricate. Its only disadvantage seems to be the amount of space it requires in the loading column. This space requirement is dictated by the volume of foam necessary to dissipate the strain energy of the system.

RECOMMENDATIONS

It is recommended that the vibration problem involving the top plate and jack be investigated further. Availability and convenience dictated the selection of springs used to damp out the induced vibration of the top plate. If a proper stiffness value was found for the springs, even greater damping could be expected. Another problem to consider when spring mounts are used is the motion of the jack relative to that of the transmission driving it. The coupling between these two components should be flexible enough to permit adequate movement of the jack.

The polyethylene foam should be used as the energy dissipating medium for the strain energy released in the tensile rod. It has adequate energy storage capacity and does not become brittle at low temperatures. It is suggested, however, that the vertical length of the shock absorber be shortened as much as possible as a matter of convenience to the operator of the testing machine.

BIBLIOGRAPHY

1. Abrahamson, H. N. H. J. Plass and E. A. Ripperger. Stress wave propagation in rods and beams In: Advances in Applied Mechanics 5:111-194. 1958.

2. Baldwin-Lima-Hamilton Corporation. Type U-1 SR-4 load cell. Philadelphia, 1951. 2 p. (Miscellaneous bulletin no. 324)

3. Chang, C. S. Energy dissipation in longitudinal vibration. In: Proceedings of the Third U. S. National Congress on Applied Mechanics, New York, 1958. New York, American Society of Mechanical Engineers, 1958. p. 109-116.

4. Crede, Charles E. and Edward J. Lunney. Establishment of vibration and shock tests for missile electronics as derived from the measured environment. Dayton, Ohio, 1956. 49 p. (U. S. Air Force, Wright Air Development Center. Technical report 56-503)

5. Davids, Norman. (ed.) International symposium on stress wave propagation in materials. New York, Interscience Publishers, 1960. 337 p.

6. Dow Chemical Company. Ethafoam - Dow expanded polyethylene. Midland, Michigan, 1960. 11 p. (Bulletin no. 171-125B-85C-461)

7. Ellis, J. T. and Stanley Karbowniczek. Absorbing shock loads for smooth, accurate stopping. Machine Design 34:176-184. Mar 15, 1962.

8. Fullman, Carl Harvey. The design of a mechanism for tensile testing in a liquid helium dewar. Master's thesis. Corvallis, Oregon State University, 1961. 91 numb. leaves.

9. Gazda, Alvin J. The buckling mode of a tension bar after the load is released. Journal of the Aerospace Sciences 29:487-488. 1962.

10. Harris, Charles O. Introduction to stress analysis. New York, Macmillan, 1961. 330 p.

11. Harris, Cyril M. and Charles E. Crede. (eds.) Shock and vibration handbook. New York, McGraw Hill, 1961. 3 vols.

12. Hartog, J. P. Den. Advanced strength of materials. New York, McGraw Hill, 1952. 379 p.

13. Hull, Gordon Laurance. The design of a variable strain rate, autographic recording, tensile testing machine. Master's thesis. Corvallis, Oregon State University, 1962. 104 numb. leaves.

14. Klumpp, James H. and Benjamin J. Lazan. Frictional damping and resonant vibration characteristics of an axial slip lap joint. Dayton, Ohio, 1954. 33 p. (U. S. Air Force, Wright Air Development Center. Technical report 54-64).

15. Kolsky, H. Stress waves in solids. Oxford, Cumberlege, 1953. 211 p.

16. Kornhauser, M. Prediction and evaluation of sensitivity to transient accelerations. Journal of Applied Mechanics, Transactions of the American Society of Mechanical Engineers 76: 371-380. 1954.

17. Kropschot, R. H. et al. Low temperature tensile testing equipment and results (300° - 20°K). 1953. 26 p. (National Bureau of Standards. Report 2708)

18. Popov, E. P. Mechanics of materials. New York, Prentice-Hall, 1952. 441 p.

19. Ripperger, E. A. The propagation of pulses in cylindrical bars - an experimental study. In: Proceedings of the First Midwestern Conference on Solid Mechanics. Urbana, Illinois, University of Illinois, 1953. p. 29-39.

20. Shigley, Joseph Edward. Machine Design. New York, McGraw Hill, 1956. 523 p.

21. Timoshenko, Steven. Vibration problems in engineering. 3d ed. Princeton, D. Van Nostrand, 1955. 468 p.

22. Tong, Kin N. Theory of mechanical vibration. New York, Wiley, 1960. 348 p.

APPENDIX

CALCULATIONS

Deflections of Testing Machine Components

Gordon Hull determined the deflections, under maximum load, for the top plate, vertical supports, reaction beam attachments reaction beam, jack screw, and adapters (13, p. 40). The deflection of the load cell is given in the data sheet accompanying the load cell (2). These deflections are tabulated on page 8 of the text.

Tensile Rod

The tensile rod, shown in Figure 25, is fabricated from 6A1 - 4Va cold rolled titanium.
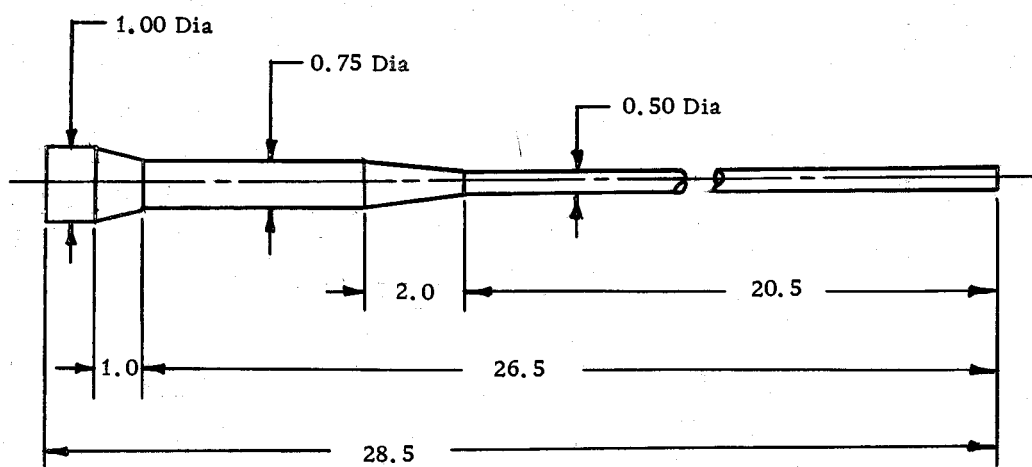

Figure 25. Tensile rod

Since the actual tensile rod is not of the same cross-sectional area along its entire length, the deflection calculations must take this fact into consideration. The equation for the longitudinal deflection of a bar having n prismatic cross-sections under an axial load is:

$$y = \frac{P}{E} \sum_{i=1}^{n} \frac{L_i}{A_i}$$

Where L_i and A_i represent the length and area of each prismatic cross-section of the bar (18, p. 34).

For titanium (8, p. 66):

$$E = 16 \times 10^6 \text{ pounds per square inch}$$

$$= 4.25 \times 10^{-4} \text{ pound seconds squared per inches to the fourth power}$$

Under a maximum load of 20,000 pounds, the longitudinal deflection of the tensile rod is approximately:

$$y = \frac{20,000}{16 \times 10^6} \left[\frac{21.5}{0.196} + \frac{5.50}{0.442} + \frac{1.50}{0.785} \right]$$

$$= 0.1565 \text{ inches}$$

Yoke Assembly

The yoke assembly is made from titanium. Its length is 1.50

inches and its average cross-sectional area is 0.540 square inches

(8, p. 73). The elongation, under maximum load, is:

$$y = \frac{PL}{AE} = \frac{(20,000)(1.50)}{(0.54)(16 \times 10^6)} = 0.0037 \text{ inches}$$

Tensile Specimen

The approximate elongation of a steel tensile specimen having

a cross-sectional area of 0.200 square inches and a length of 4.50

inches is:

$$y = \frac{PL}{AE} = \frac{(20,000)(4.50)}{(0.20)(30 \times 10^6)} = 0.0150 \text{ inches}$$

Compressive Column

The compressive column is made from type 304 stainless steel

tubing having a length of 28.5 inches, an outside diameter of 1.88

inches, an inside diameter of 1.71 inches, and a cross-sectional

area of 0.445 inches (8, p. 67). Under maximum load it is com-

pressed an amount:

$$y = \frac{PL}{AE} = \frac{(20,000)(28.5)}{(0.445)(30 \times 10^6)} = 0.0426 \text{ inches}$$

Strain Energy in Loading Column

Under a maximum load of 20,000 pounds the total elongation

of the part of the loading column in tension is:

$$y = (0.0040 + 0.0028 + 0.0050 + 0.0018 + 0.1565 +$$

$$0.0037 + 0.0100)$$

$$= 0.1856 \text{ inches}$$

The strain energy present in this part of the loading column is then:

$$W = \frac{Py}{2} = \frac{(20,000)(0.1856)}{2} = 1856 \text{ inch-pounds}$$

Similarly, the strain energy present in the loading column between the load cell and the tensile specimen is:

$$W = \frac{Py}{2} = \frac{(20,000)}{2}(0.0018 + 0.1565 + 0.0037 + 0.0100)$$

$$= 1720 \text{ inch-pounds}$$

The percent of total strain energy acting on the load cell that this part of the system represents is:

$$\text{Percent } W = \frac{1720}{1856}(100 \text{ percent}) = 92.6 \text{ percent}$$

Response of Tensile Rod

Theoretical Calculations

From the equations derived in the text of the thesis the frequency of the fundamental mode was found to be:

$$f_1 = \frac{c}{4L}$$

For titanium:

$$c = \sqrt{\frac{E}{\rho}} = \sqrt{\frac{16 \times 10^6}{4.25 \times 10^{-4}}} = 194,000 \text{ inches per second}$$

The length of the tensile rod assembly is 30.8 inches. Its fundamental frequency is then:

$$f_1 = \frac{194,000}{(4)(30.8)} = 1570 \text{ cycles per second}$$

Experimental Calculations

In Figure 6, the fundamental frequency is:

$$f_1 = \frac{n \text{ cycles of fundamental frequency}}{\left[\begin{array}{l} \text{number of units along time axis} \\ \text{needed to complete } n \text{ cycles} \end{array}\right] \left[\frac{\text{number of seconds}}{\text{unit}}\right]}$$

$$= \frac{2 \text{ cycles}}{(18.5 \text{ units})(10^{-4} \frac{\text{seconds}}{\text{unit}})}$$

$$= 1080 \text{ cycles per second}$$

Energy Dissipation Per Cycle

The relationship between strain energy and applied load has been stated in the text of the thesis as:

$$W = \frac{P^2 L}{2AE}$$

Referring to Figure 6, if the magnitude of each successive maximum

compressive load is obtained, the strain energy remaining in the

tensile rod at that time can be calculated from the above equation.

Since the cross-sectional area of the tensile rod assembly is

not constant, an equivalent cross-sectional area should be found so

that the above equation can be applied. The tensile rod assembly was

weighed and found to be 1.60 pounds. The density of titanium is

0.160 pounds per cubic inch. The volume of the tensile rod assembly

is:

$$V = \frac{weight}{density} = \frac{1.60}{0.160} = 10.0 \text{ cubic inches}$$

The length of the assembly is 30.8 inches. The equivalent cross-

sectional area is then:

$$A = \frac{V}{L} = \frac{10.0}{30.8} = 0.325 \text{ square inches}$$

The strain energy in the tensile rod assembly, for an applied load of

P, is:

$$W = \frac{(30.8) P^2}{(2)(0.325)(16 \times 10^6)} = 2.96 \times 10^{-6} P^2 \text{ inch-pounds}$$

The maximum compressive load for the first cycle is 4400

pounds. The strain energy in the tensile rod assembly at that time

is then:

$$W = (2.96 \times 10^{-6}) (4400)^2 = 83.0 \text{ inch-pounds}$$

The maximum compressive loads for the second and third

cycles are 2800 and 1500 pounds respectively, and their correspond-

ing strain energies are 31.0 and 9.4 inch-pounds. Thus, between the

first and second cycle:

$$\text{Percent energy loss} = \left[\frac{83.0 - 31.0}{83.0}\right] \text{ (100 percent)}$$

$$= 62.6 \text{ percent}$$

Similarly, between the second and third cycles:

$$\text{Percent energy loss} = \left[\frac{31.0 - 9.4}{31.0}\right] \text{ (100 percent)}$$

$$= 69.6 \text{ percent}$$

The average percent energy loss per cycle for the first three cycles

is:

$$\frac{62.6 + 69.6}{2} = 66.1 \text{ percent}$$

Response of Load Cell

Theoretical Calculations

Applying the same analysis used for the tensile rod the theoret-

ical fundamental frequency of the load cell can be calculated. For

steel, $c = 202,000$ inches per second (10, p. 206). The length of

the load cell is 8.5 inches. The fundamental frequency is then:

$$f_1 = \frac{c}{4L} = \frac{202,000}{(4)(8.5)} = 5940 \text{ cycles per second}$$

Experimental Calculations

Using Figure 7 and the same procedure as for the tensile rod, the actual fundamental frequency of the load cell is:

$$f_1 = \frac{n \text{ cycles of fundamental frequency}}{\left[\begin{array}{l}\text{number of units along time axis} \\ \text{needed to complete } n \text{ cycles}\end{array}\right] \left[\frac{\text{number of seconds}}{\text{unit}}\right]}$$

$$f_1 = \frac{6 \text{ cycles}}{(19.5 \text{ units}) (10^{-4} \frac{\text{seconds}}{\text{unit}})}$$

$$= 3250 \text{ cycles per second}$$